BEHAVIOR OF GRANULAR COLUMN SUPPORTED GABION-RAFT FOUNDATION

Thesis submitted in partial fulfillment of the requirement for the degree of

Master of Civil Engineering
In
Soil Mechanics and Foundation Engineering

By

Shubhadip Sen

Roll No.: 002110402009
Examination Roll No.: **M4CIV23002B**
Registration No. **160031** of **2021-2022**

Under the guidance of

Dr. Arghadeep Biswas
Assistant Professor
Department of Civil Engineering
Jadavpur University
Kolkata - 700032

and

Dr. Obaidur Rahaman
Assistant Professor
Department of Civil Engineering
Jadavpur University
Kolkata – 700032

Department of Civil Engineering
Faculty of Engineering & Technology
Jadavpur University
Kolkata – 700032
November, 2023

DECLARATION OF ORIGINALITY AND COMPLIANCE OF ACADEMIC ETHICS

This is to declare that I, **Shubhadip Sen**, student of Geotechnical Engineering Division of the Department of Civil Engineering, class roll no. **002110402009**, have prepared this thesis entitled "**BEHAVIOR OF GABION-RAFT FOUNDATION SUPPORTED BY GRANULAR COLUMNS**" under the supervision of Dr. Arghadeep Biswas and Dr. Obaidur Rahaman. This manuscript is original and not directly plagiarized in any sense. However, the Literature studied for the preparation of this report has been cited wherever required and also presented in the list of references.

Date:

Shubhadip Sen
Roll No. : 002110402009
Department of Civil Engineering
Jadavpur University, Kolkata

CERTIFICATE

This is to certify that the thesis entitled **"BEHAVIOR OF GRANULAR COLUMN SUPPORTED GABION-RAFT FOUNDATION"** has been carried out by **Shubhadip Sen** bearing Class Roll No: **002110402009**, Examination Roll No.: **M4CIV23002B** and Registration No: **160031 of 2021-2022**, under our guidance and supervision and be accepted in partial fulfillment of the requirement for the degree of Master of Engineering in Soil Mechanics and Foundation Engineering in the Department of Civil Engineering.

Dr. Arghadeep Biswas
Assistant Professor
Department of Civil Engineering
Jadavpur University
Kolkata - 700032

Dr. Obaidur Rahaman
Assistant Professor
Department of Civil Engineering
Jadavpur University
Kolkata – 700032

Head of the Department
Department of Civil Engineering
Jadavpur University
Kolkata - 700032

Dean
Faculty of Engineering and Technology
Jadavpur University
Kolkata – 700032

FACULTY OF ENGINEERING & TECHNOLOGY

JADAVPUR UNIVERSITY

CERTIFICATE OF APPROVAL

The forgoing thesis titled **"BEHAVIOR OF GRANULAR COLUMN SUPPORTED GABION-RAFT FOUNDATION"** is hereby approved as a creditworthy study of an engineering subject conducted and presented satisfactorily to warrant its acceptance as a precondition to the degree for which it was submitted. It is understood that the undersigned does not automatically support or accept any argument made, opinion expressed, or inference drawn in it by this approval, but only approves the thesis for the reason it was submitted.

Committee on Final Examination for Evaluation of the Thesis

_____

Signature of External Examiner

_____ _____

Signature of Supervisor **Signature of Supervisor**

ACKNOWLEDGEMENT

I, Shubhadip Sen, bearing Roll No. 002110402009 would like to take this opportunity to thank my supervisors, Dr. Arghadeep Biswas and Dr. Obaidur Rahaman, for their constant guidance and support without which this work wouldn't have been possible. I would also like to thank Prof. Ramendu Bikas Sahu, Prof. Sibapriya Mukherjee (Retd.), Prof. Gupinath Bhandari, Prof. Sumit Kr. Biswas, and Prof. Narayan Roy, who have imparted valuable knowledge throughout the course.

I would be failing in my duties if I didn't thank my classmates, especially Ajfar and Subhadeep. Constant discussion with them uplifted the quality of this work significantly.

For Maa and Baba, who have consistently been my source of unwavering support, expressing sufficient gratitude would always fall short.

Date:

Place: Jadavpur

Shubhadip Sen

ABSTRACT

Soft clays exhibit insufficient bearing capacity and experience excessive settlement under load. To mitigate these effects, various ground improvement techniques are employed, with Granular Columns being a commonly used and effective approach. They are frequently implemented in soft clayey soils to enhance the bearing capacity of the native soil between the columns and promote pore water pressure dissipation through soil squeezing. However, in very soft clays, stone columns can lose their structural integrity and encounter drainage issues due to clogged voids at the clay-column interface. To address these limitations, the Ordinary Stone Column (OSC) technique was modified by encasing the granular materials within a Geogrid Encasement. This modification improves the bearing capacity of the encased stone columns without compromising their drainage capacity. Furthermore, the inclusion of a gabion on top of the stone columns, consisting of granular materials enclosed within geogrid, helps distribute the load evenly among the stone columns.

In this study, a comprehensive investigation has been conducted using FE analysis with PLAXIS3D. The problem geometry has been modeled as a 3D strip in PLAXIS, and a parametric study has been performed to analyze the impact of various factors such as the properties of the soft soil (c and ϕ), angle of friction of the stone column material (ϕ), length of encasement, column spacing, geogrid and gabion stiffness, and embankment material density. This analysis aims to enhance our understanding of the physical performance of the stone columns in different scenarios.

TABLE OF CONTENTS

LIST OF FIGURES

LIST OF TABLES

NOTATIONS AND ABBREVIATIONS

A_s	Surface Area of Side
A_c	Cross sectional area of the Column
c_u	Undrained Cohesion
c'	Drained Cohesion
c_r	Pseudo-Cohesion developed due to the confinement encasement
$\bar{c}$	Average Cohesion
K_p	Coefficient of Passive Earth Pressure
$\Delta\sigma_3$	Additional Confining Pressure Due to the Confinement
M	Secant Modulus of the geocell material
N_0	Bearing Capacity Factor
ε	Axial Strain
D	Initial Diameter of the geocell
σ_{rL}	Total Limiting Radial Stress
σ_{ro}	Initial Effective Radial Stress
u_o	Initial excess pore pressure
n	Stress Concentration factor
σ_s	Stress in Column-Surrounding Cohesive soil
μ_c	Ratio of stresses in Clay
μ_s	Ratio of stresses in Stone Column
σ_c	Stress in the Stone Column
ϕ'	Drained Friction Angle of Soft Clay
γ_{sat}	Saturated Unit Weight
E'	Drained Elastic Modulus
k_h	Coefficient of Horizontal permeability
C_c	Coefficient of Compression
C_s	Coefficient of Swelling
e_0	Initial Void Ratio
k_v	Coefficient of Vertical permeability
ϕ_{clay}	Internal angle of Friction for soft soil
ϕ_{sc}	Internal angle of Friction for granular column material
J_{sc}	Stiffness of Encasement Geogrid
J_{gab}	Stiffness of Gabion Geocell
ESC	Encased Stone Column
FEA	Finite Element Analysis
OSC	Ordinary Stone Column
OCR	Over Consolidation Ratio

INTRODUCTION

1.1 GENERAL

India, among other countries, possesses vast expanses of weak clay. Particularly along the coastlines. These expanses are generally characterised by very weak load bearing capacity and excessive settlement. And thus, rendered unsuitable for any form of activity; be it commercial or for residential purposes. Although the use of pile foundation can meet all the design requirements, large length of the pile required often results in exorbitantly high costs. Given these circumstances, Engineers are increasingly considering the use of ground improvement techniques for its economic viability. Several ground improvement techniques have been devised till date. These may include, for instance, soft soil replacement, basal embankment reinforcement, use of lightweight fill material, prefabricated vertical drains and surcharge or vacuum to accelerate settlements, staged construction, or injection of soil cement mixture. Stone columns, among other methods, are commonly employed for ground improvement. This ground improvement technique has been successfully applied to increase the bearing capacity and to reduce the settlement for foundation of structures like liquid storage tanks, earthen embankments, raft foundations, etc., where a relatively large settlement is permissible. Stone columns have also been used to improve slope stability of embankments on soft ground

The concept of stone columns was first utilized in France in 1830 to enhance the quality of natural soil. Since the pioneering work of Greenwood (1970), Stone columns have been employed worldwide in challenging foundation sites to enhance bearing capacity, mitigate total and differential settlements, expedite consolidation, improve slope stability of embankments, and enhance resistance to liquefaction (Barksdale and Bachus 1983; Alamgir et al. 1996).

When stone columns are installed in very soft clays (undrained cohesion, c_u<10 kPa) without sufficient confinement, the stones within the column may be forced out, resulting in loss of stone. This requires a larger quantity of stones to form the column. Moreover, the fine particles from the surrounding soft clay tend to mix with the aggregates which causes reduction in the frictional properties and the drainage function of the column. The load-bearing capacity of the stone columns which primarily relies on the shear strength of the surrounding clayey soil limits their ability to improve beyond approximately 8 times the strength of the soft clay, as noted by Chummar (2000) and Thorburn (1975). Additionally, Ordinary Stone Columns (OSC) are unsuitable for higher loads as they tend to fail by bulging. These limitations can be overcome

by enclosing the stone column with an appropriate geosynthetic material and formulating an Encasing Stone Column (ESC).

Previous studies have obtained valuable findings for a deep understanding of ground improvement using stone columns. However, most of these studies have been conducted from the viewpoint of measuring the relative improvement in the performance of ESC and OSC. Also, gabions have been used extensively as retaining structures, and their effectiveness is well documented. However, the conjugation of stone columns with flexible gabions into a single foundation system remains an unexplored domain. In this study, the combined behavior of a flexible gabion and ESC will be examined and their effectiveness in the working system will be evaluated. The numerical model will be generated with the help of Finite Element Analysis (FEA) software PLAXIS 3D. A parametric study will then be conducted to study the influencing factors on the settlement behavior of the soft subgrade.

1.1.1 *Ordinary Stone Columns*

Stone columns are utilized as a means of reinforcing soil by introducing additional stiffness, strength, and load-bearing capacity to the surrounding area. They play a significant role in enhancing the shear strength of the soil. When stone aggregates are compacted and installed, they interlock with the adjacent soil particles, resulting in an increase in frictional resistance between them. This interlocking mechanism boosts the shear strength of the soil. Additionally, stone columns act as vertical load-bearing elements, transferring the load from structures or foundations to deeper and more competent soil layers. This distribution of load reduces stress on weaker and less competent soil layers, resulting in reduced settlement and increased bearing capacity of the improved ground.

The installation of stone columns creates a confinement effect on the surrounding soil which compacts the soil laterally. Therefore, the density, and stiffness of soil are enhanced. This confinement effect further improves the load-bearing capacity, and overall stability of the soil. Furthermore, stone columns can enhance the drainage characteristics of the soil. The gaps or voids between the stone aggregates allow for improved water flow, reducing excess pore pressure and increasing effective stress. This improved drainage helps to prevent excessive settlement and potential soil liquefaction in saturated or loose soils.

Over time, stone columns may undergo consolidation, resulting in gradual densification and settlement of the soil and stone column system under sustained loads. Time consolidation contributes to the long-term stability and overall performance of the soil. In summary, the

presence of stone columns reinforces the soil, increasing its load-bearing capacity, reducing settlement, and enhancing overall stability. The specific effects of stone columns as soil reinforcement depends on various factors such as column spacing, diameter, length, and properties of the surrounding soil. Proper design, installation, and monitoring are essential to achieve the desired soil improvement and reinforcement goals. Several construction projects utilizing stone columns have been documented by Hughes and Withers (1974), Hughes et al. (1975), Mitchell and Huber (1985), and others.

1.1.2 *Encased Stone Columns*

McKenna et al. (1975) reported a case history where the stone column was not adequately confined by the surrounding soft clay. As a result, there was excessive bulging and the soft clay infiltrated into the gaps within the aggregate. In such scenarios, in order to enhance its performance, it is necessary to provide additional confinement to the stone column. Encased stone columns, also referred to as stone column encasement or stone column jacketing, are a modified version of the conventional stone column ground improvement method. In this approach, the stone columns are surrounded by a geosynthetic encasement, typically made of geotextile or geogrid fabric. The purpose is to augment their load-bearing capacity and enhance the overall performance of the ground. Encasing the stone column within a geosynthetic material provides additional confinement to both the column and the surrounding soil. This confinement aids in distributing the load more uniformly along the stone column and improves the lateral confinement of the soil. Consequently, the load-bearing capacity increases, and settlement of the treated ground reduces. The geosynthetic encasement enhances the interaction between the stone column and the adjacent soil. It improves the frictional resistance between them, thereby elevating the shear strength and stability of the ground. Additionally, the geosynthetic encasement serves as a filtration and drainage layer. It permits water to pass through the stone column while preventing the migration of fine soil particles into the column. This maintains the desired drainage characteristics of the treated ground. Encased stone columns outperform traditional stone columns by providing additional confinement and enhancing the load-bearing capacity of the soil. The design and installation of encased stone columns require careful consideration of various factors, including column spacing, diameter, length, properties of the geosynthetic encasement, and soil conditions in the vicinity. It is crucial to employ proper design and construction techniques to ensure the successful implementation of encased stone column ground improvement projects.

1.1.3 *Gabion*

A gabion is a rectangular or cylindrical wire mesh basket or container filled with stones, rocks, or other materials. It is commonly used in civil engineering and construction projects for various purposes, including erosion control, retaining walls, and bank stabilization. Gabions offer several advantages in construction projects. They provide effective erosion control by stabilizing slopes and preventing soil erosion caused by water flow. They also act as retaining structures, holding back soil or other materials to create terraces or level surfaces. Additionally, gabions are often used in the construction of flood barriers and channel linings, as they allow water to pass through while reducing the force of the water flow.

Although gabions are primarily used as retaining structures, using them as flexible padding in place of regular sand pads can reduce settlement. Latha (2007), showed that when granular materials are encased, a pseudo-cohesion is developed due to the confinement developed from the encasement, as given in Eq. 1.1.

$$Cr = \frac{\Delta\sigma_3\sqrt{Kp}}{2} \tag{1.1}$$

where K_p is the coefficient of passive earth pressure and $\Delta\sigma_3$ is the additional confining pressure due to the confinement as shown in Eq. 1.2.

$$\Delta\sigma_3 = \frac{2M[(1-\sqrt{1-\varepsilon})]}{D(1-\varepsilon)} \tag{1.2}$$

where ε is the axial strain at failure state; M is the secant modulus of the geocell material at the axial strain of ε, and D is the initial diameter of the geocell.

1.2 MOTIVATION AND OBJECTIVE OF THE STUDY

It was Greenwood (1970) who first introduced the idea of using stone columns to improve the performance of soft soil. Over the years, there has been extensive research on the use of stone columns for ground improvement. Hughes et al. (1975) conducted a study that established a relationship between the load applied and the settlement for an isolated stone column in soft clay when subjected to plate loading. Goughnour and Bayuk (1979) and Aboshi et al. (1979) investigated stress concentration in systems where a stone column was embedded in soft soil. Their research revealed that when loaded, stress accumulates within the stone column, while the surrounding, less rigid soil experiences reduced stress. Barksdale and Bachus (1983) were the first to create an idealized unit cell model of the stone column-soft clay system. They demonstrated that the stress concentration factor, denoted as 'n,' can be predicted using elastic

theory as a function of the modular ratio of the stone and clay, assuming equal vertical displacements. Ambily and Gandhi (2007) conducted a comprehensive experimental investigation on both single columns and groups of seven columns. Their findings indicated that when only the column area is loaded, failure occurs through bulging, with the most significant bulging observed at a depth approximately 0.5 times the diameter of the stone column. The study also suggested that as the spacing between columns increases, the axial capacity of the column decreases, and settlement increases until an s/d ratio of 3 is reached, beyond which any further change becomes negligible.

However, in cases where stone columns are installed in extremely soft soils, their ability to support heavy loads may be limited due to insufficient lateral soil confinement. McKenna et al. (1975) documented instances where stone columns were not adequately constrained by the surrounding soft clay, leading to excessive bulging and the infiltration of soft clay into the voids within the stone aggregates. This phenomenon ultimately reduced both the bearing capacity and drainage efficiency of the stone columns. The concept of encased granular columns gained populace over the years. Raithel (1999) established that the confining pressure in the geo-encasement is not solely determined by hoop strength at failure but also depends on the tensile stiffness modulus. Building on this research, Raithel and Kempfert (2000) conducted a numerical study on granular columns using the soft soil model (SSM) for the soft clay and the hard soil model (HSM) for the column material. This study provided detailed guidelines for designing the ESC (encased stone column).

The existing literature were thoroughly studied and analyzed and and have been summarized in chapter 2. It can be ascertained that encased stone columns offer a significant improvement in performance over ordinary stone columns. This can be attributed to the confinement offered by the encasement. This hoop stress thus developed plays a crucial role in reducing the vertical stress in the column. Also load bearing platforms of some form have been used hand-in-hand with granular columns in order to facilitate in a more efficient load distribution. In this present study, the load distribution platform have been emulated by a gabion.

During the review, it was found out that most of the work published aimed at the performance of singular OSC or ESC. However, where the 3D strip model have been used, sand pads have been the most common form of load bearing platform. The use of flexible gabions as load bearing platform remained an unexplored domain. However, it was seen that gabions have been extensively used in retaining structures and some references has been drawn from the same.

This study envisages to present all overall study of the ESC-Gabion foundation system. The broad objectives of this study have been listed below.

- To formulate a numerical model of the ESC-Gabion foundation system and perform finite element analysis using FEA Package, PLAXIS 3D.
- To assess the pore pressure development, vertical deformation and lateral displacement under the influence of embankment loading.
- To perform an extensive parametric investigation aimed at evaluating how the cohesion of clay, spacing of granular columns, Length of encasement and stiffness of the geogrid affects the overall performance of the ESC-Gabion foundation system.

1.3 ORGANIZATION OF THE THESIS WORK

The thesis will be broken down into several chapters for an easier breakdown of the work. Initially, the work plan for the 5 chapters is finalized as described below.

Chapter 1 serves as an introduction to the entire thesis.

In **Chapter 2**, selected studies on OSC, ESCs, and gabion are presented. The chapter concludes with the summarization of the literature reviewed and the detailed scope of the present study.

Chapter 3 deals with the materials and methodology adopted for the study. Details of soil parameters used, the geometric model developed, the selection of model parameters, mesh fineness, and FE analysis are detailed in this chapter.

The results obtained from the analysis performed are elaborated in **Chapter 4.** Various key factors related to the study are discussed with possible mechanisms involved. Analysis of the parameters which affect the performance most significantly have also been done and thus documented.

Chapter 5 covers the statistical analysis performed on the results obtained. This chapter presents the summary, conclusions, limitations, and scope of future study. It will also present a summary of the present research and conclusions drawn from the obtained results and documents some suggestions on the scope of future study in the related field.

LITERATURE REVIEW

2.1 INTRODUCTION

In this section, a compilation of past research studies focusing on ground modification using stone/granular columns and geosynthetic-encased stone columns is presented. Additionally, this review work includes studies on gabion structures, although their primary use appears to be for retaining backfills. These studies have provided valuable insights into the behavior of ordinary stone columns (OSC) and encased stone columns (ESC). The research findings have demonstrated the effectiveness of OSC and ESC compared to other ground improvement techniques. This chapter of the literature review aims to identify the progress made in this field and critically evaluate the findings to identify future research opportunities.

2.2 LITERATURE REVIEW

2.2.1 *Ordinary stone columns*

Greenwood (1970) introduced the concept of utilizing stone columns to enhance soft soil by minimizing settlement. The arrangement of these stone columns is typically established based on acceptable settlement limits for the anticipated loads, as well as to ensure comprehensive coverage of the ground area through overlapping zones. Additionally, the spacing between the columns depends on the desired level of improvement necessary to establish a reliable foundation under the designated design load. Practical experience has shown that closer spacing between the columns is generally preferred when dealing with individual footings as opposed to larger rafts.

Bauman and Bauer (1974) and **Mitchell** (1981) conducted research on the practical implementation of stone column construction. Their studies demonstrated that the vibro-floatation method, commonly used for constructing stone columns in soft clay, can be modified into a vibro-replacement method. This modification has gained widespread acceptance and is extensively employed in the construction of stone columns. **Aboshi et al**. (1979), **Nayak** (1996) and **Datye and Nagaraju** (1975) were few among others who have worked on developing an effective methodology towards constructing stone columns.

Hughes et al. (1975) in their study established a load-settlement relationship for plate loading of an isolated stone column in soft clay. It was assumed that vertical shear stress developed along the side of the column is equal to the average shear strength of the soil when end bearing failure is about to occur, the critical length can be evaluated by equating the boundary forces on the column; Eq. 2.1 depicts that column load equals the sum of shaft friction resistance and end bearing force.

$$p = \overline{c}As + N_o cAc \tag{2.1}$$

Where, p is the ultimate column load, N_o is the appropriate bearing capacity factor (taken 9 for a long column), A_s is the surface area of the side of the column, and A_c is the cross sectional area of the column.

The total limiting radial stress (σ_{rL}) is calculated as,

$$\sigma_{rL} = 4c + \sigma_{ro} + u_o \tag{2.2}$$

where σ_{ro} is the initial effective radial stress and u_o is the initial excess pore pressure.

In their studies, **Goughnour and Bayuk** (1979), as well as **Aboshi et al.** (1979), investigated stress concentration in the system comprising a stone column embedded in soft soil. When the ground reinforced with stone columns is subjected to loading, there is an accumulation of stress within the stone column, while the surrounding soil, which is comparatively less rigid, experiences a reduction in stress. The vertical stress distribution within a unit cell can be quantified using a stress concentration factor denoted as 'n', which represents the ratio of stress in the stone column (σ_c) to the stress in the cohesive soil surrounding it (σ_s).

$$n = \frac{\sigma_s}{\sigma_c} \tag{2.3}$$

The magnitude of stress concentration depends on the relative stiffness of the stone column and the surrounding soil. The value of n is generally lies between 2 and 6, with the value of 3–4, at the ground surface.

Barksdale and Bachus (1983) were the first to make unit cell idealization of the stone column-soft clay system. They showed that the stress concentration factor, n, may be predicted using elastic theory as a function of the modular ratio of the stone and the clay, assuming equal vertical displacements. The stress in the clay and stone using the stress concentration factor n is calculated using the following two equations.

$$\sigma_c = \frac{\sigma}{[1 + (n-1)a_s]} = \mu_c \sigma \tag{2.4}$$

$$\sigma_s = \frac{n\sigma}{[1 + (n-1)a_s]} = \mu_s \sigma \qquad (2.5)$$

where, n is the stress concentration factor and μ_c and μ_s are the ratio of stresses in clay and stone respectively, respectively, to the average stress σ over the tributary area. This study also shed some valuable light on the failure mechanism of the stone columns. Failure takes place primarily by bulging. Short columns however undergo shear failure or punching failure based on the rigidity of the material at the base of the column.

The research conducted by **Priebe** (1995) focused on the impact of the compressibility of column material and the overburden. Priebe (1995) developed a set of design charts that enable the estimation of settlement for single and strip footings reinforced with a restricted number of stone columns. These charts provide a means to derive Priebe's "basic improvement factor". It is important to note that Priebe's formulation assumes that the columns terminate at a rigid layer. Consequently, this method is not applicable for predicting the behaviour of floating columns. The volume of soil replaced by stone columns has an important effect on the performance of the improved ground. To quantify the amount of soil replacement, the Area Replacement Ratio, a_s, is defined as the ratio of the area of the stone column after compaction (A_s) to the total area within the unit cell (A). **Shahu et al.** (2000) showed that increasing the area ratio improves the overall response of granular pile-reinforced ground. **Wood et al.** (2000) deduced that a significant improvement in bearing capacity for stone column-treated ground requires an area replacement ratio of 0.25 or greater.

Ambily and Gandhi (2007) conducted a comprehensive experimental investigation on both a single column and groups of seven columns. Their objective was to examine the achieved improvement and measure the stress intensity on the column and the soil. To do so, they utilized pressure cells attached to the loading plate and compared the obtained results with those obtained through the finite element package of PLAXIS 2D. The findings of the study indicated that when solely the column area is loaded, failure occurs through bulging, with the most significant bulging observed at a depth approximately 0.5 times the diameter of the stone column. Additionally, the study inferred that as the spacing between columns increases, the axial capacity of the column decreases, and settlement increases until an *s/d* ratio of 3 is reached, beyond which any further change becomes negligible. The extent of ground

improvement was summarized through a curve that establishes a correlation between the stiffness improvement factor β, *s/d* ratio, and ϕ of the stone column material.

Ng and Tan (2014) simplified the design method for stone columns by introducing the Equivalent Column Method (ECM). This method involves developing equivalent stiffness and permeability parameters based on the characteristics of the soft clay and stone column. By doing so, the stone column and surrounding soil system can be replaced with an equivalent soil having the same parameters. One advantage of this approach is that it eliminates the need to individually design each stone column, thereby saving time. The effective parameters can be readily determined using the charts provided in the paper. To validate the suitability of the ECM model for modeling stone columns, a comparison was made with a plane strain model. The pore pressure dissipation patterns and settlement characteristics were found to be in agreement, thus confirming the effectiveness of the ECM model. However, a limitation of the ECM model is that it assumes the stone column behaves as a linearly elastic material. In reality, after bearing the initial load, the stone column undergoes plastic deformation and bulges outward.

Vinoth et al. (2019) presented three distinct approaches for modeling stone columns, namely the enhanced soil parameter, equivalent column method, and embedded beam method. These approaches collectively emphasize that the individual parameters of the soft soil and soil column have limited significance, as it is the combined equivalent parameter that governs the overall properties. The study collected real-life data from a road pavement project in Mumbai and adopted staged construction for the PLAXIS 2D simulations. The stone columns were initially installed through soil replacement, followed by the application of embankment load in subsequent stages. In the final phase, consolidation was conducted until the pore pressure reached 1 kPa. However, the results obtained at the conclusion of the study exhibited significant deviations from the actual field data. These discrepancies could be attributed to the absence of a sand crust layer, which helps distribute the load evenly among the stone columns. Furthermore, the soil models employed in the study, specifically the hardening soil model and soft soil model for fill material and soft clay, added complexity to the calculation process. Consequently, several researchers have recommended utilizing the Mohr-Coulomb Model for more efficient and time-saving analysis.

2.2.2 *Encased Stone Columns*

In situations where stone columns are installed in highly soft soils, their ability to bear substantial loads may be limited due to inadequate lateral soil confinement. **McKenna et al.** (1975) documented instances where the stone columns were not properly constrained by the surrounding soft clay, resulting in excessive bulging and the soft clay infiltrating the voids within the stone aggregates. This phenomenon ultimately diminished both the bearing capacity and drainage efficiency of the stone columns.

Ghionna and Jamiolkowski (1981) and **Van Impe and Silence** (1986) were among the early researchers who acknowledged the potential of encasing columns with geotextiles. They developed an analytical design method to determine the necessary tensile strength of the geotextiles, specifically for an ultimate limit state (ULS) analysis.

Raithel (1999) established that the confining pressure in the geo-encasement is not only a function of hoop strength at failure but also depended on tensile stiffness modulus. The study was carried forward and a numerical study by **Raithel and Kempfert** (2000) was conducted on the granular column using the soft soil model (SSM) for the soft clay and hard soil model (HSM) for the column material. This study provided a detailed description of the design procedures to be followed while designing the ESC.

Malarvizhi and Ilamparuthi (2007) conducted a parametric study focusing on encased stone columns. They varied several parameters, including the length-to-diameter (*L/D*) ratio, stiffness of the geogrids used for encasing, and the internal friction angle of the stone infill material. The study utilized FEM software, PLAXIS3D, to analyze the influence of these parameters on the Settlement Reduction Ratio (*SRR*). The findings revealed that increasing the *L/D* ratio led to a reduction in settlement, but this effect was limited when the *L/D* ratio reached 10. Similarly, the stiffness of the geogrids showed a similar trend, with an enhanced performance in terms of settlement reduction observed up to a stiffness (E-value) of 2000 $kN/m^2/m$. The study also emphasized the importance of adequately compacting the in-filled material to achieve a higher degree of internal friction, as it significantly increased the efficiency of the encased stone column. It was observed that the stress concentration was higher in the encased stone column compared to a conventional stone column (OSC), and the bulging of the stone column was effective up to a depth of 4D from the top of the granular column.

In their paper, **Murugesan and Rajagopal** (2010) conducted load tests on both singular and group geosynthetic encased stone columns. The study revealed the significant influence of encasement stiffness in both cases. Additionally, it was observed that the advantage of using encasement decreases as the column diameter increases. However, the main focus of the paper lies in the detailed design procedure and the charts developed by the authors, which aids in selecting the appropriate encasement.

Pulko et.al. (2011) suggested that the dilation of the column material has a beneficial effect on settlement reduction. However, it was further mentioned that it can be neglected in the case of conservative predictions while performing numerical analysis.

Fattah and Majeed (2012) conducted a comparative analysis between ordinary stone columns (OSCs) and encased stone columns (ESCs), while also exploring the impact of a stone cap positioned above the stone column and beneath the foundation. The study utilized CRISP 2D, a two-dimensional finite element program, for the analysis.

In their paper, **Tandel et. al.** (2013) provided a detailed description of the Finite Element Analysis (FEA) process using PLAXIS 3D. Various parameters were investigated in this study, including the spacing of geosynthetic-encased stone columns (GRSC), denoted as *S*, the deformation modulus of the stone column (E_{sc}), the deformation modulus of the embankment fill (E_{fill}), the height of the embankment (h), the thickness of the soft clay (H), and the stiffness of the geosynthetic (J). The overall improvement was formulated with the help of a Settlement Improvement Factor (SIF) as follows

$$SIF = 1.4997t + 7.071\left(\frac{S}{d}\right)^{-0.19\ln(t)-0.9806} \quad (2.6)$$

Where *S/D* represents the stone column spacing to diameter ratio, and t is a non-dimensional parameter relating to the geosynthetic stiffness, stone column diameter, and soil modulus.

Rajagopal and Mohapatra (2016) conducted a comprehensive analysis of embankments supported by geosynthetic encased stone columns. Initially, it was anticipated that a slip circle would develop, leading to a failure plane. However, through detailed numerical analysis, it was revealed that no continuous slip circle was formed. Consequently, instead of employing the conventional slip circle analysis, a continuum approach utilizing numerical methods was utilized for slope stability analysis in such cases.

Rajagopal and Jayapal (2018) conducted a comprehensive review of both numerical and analytical studies related to Encased Stone Columns (ESC), delving into the subject matter in

great detail. Their findings indicated that smaller diameter encased columns exhibited better performance compared to larger diameter ones. While full encasement significantly improved settlement characteristics, partial encasement was often found to be sufficient.

The study also highlighted certain limitations of ordinary stone columns (OSC) when used in very soft clay with a low undrained cohesion (c_u < 10 kPa). In such cases, the stones of the OSC tended to squeeze out due to inadequate lateral confinement. Additionally, fine clay particles were observed to block the voids within the stone column, thereby reducing its effectiveness as a vertical drain. The strength of OSC primarily relied on the shear strength of the surrounding clay. The ultimate load carrying capacity improvement achieved with OSC was found to be limited to approximately eight times the native strength of the soft clay.

In their study, **Hosseinpour et al.** (2019) conducted a numerical analysis to examine a test embankment supported by geotextile encased columns (GECs). They compared the results of a three-dimensional (3D) analysis with those obtained from two-dimensional (2D) axisymmetric and plane strain analyses. The test embankment was constructed on a soft clay deposit in Rio de Janeiro, Brazil. The embankment had a height of 5.3m, and the soft soil was reinforced with stone columns measuring 0.8m in diameter and spaced 2m apart from each other. To account for symmetry, the stone columns were represented as semi-circular cylinders.

The settlement and pore water pressure observed aligned with the field data, indicating agreement. Based on this, the researchers concluded that axisymmetric analysis is generally a fast and useful method for estimating maximum embankment settlement, stress distribution beneath the embankment, and encasement force in GECs. On the other hand, PS analysis may be employed when computing horizontal soil deformation or conducting long-term stability analysis. While a comprehensive or strip 3D analysis can provide all the necessary information, it is time-consuming, especially when dealing with embankments supported by a large number of GECs.

Gao et al. (2020) presented a practical case study of an embankment constructed on soft soil in China. The paper focused on the effectiveness of using a geocell-reinforced granular bed to mitigate total settlement after construction. The study also investigated the impact of varying the length of the encasement to determine the most optimal length.

$$c_r = \frac{\Delta\sigma_3\sqrt{Kp}}{2} \tag{2.7}$$

$$\Delta\sigma_3 = \frac{2M[(1-\sqrt{1-\varepsilon})]}{D(1-\varepsilon)} \quad (2.8)$$

In the geocell-reinforced sand layer, cohesion was induced and denoted as "C_r" specified by Eq. 2.8 This induced cohesion was calculated using the coefficient of passive earth pressure (K_p) and the additional confining pressure ($\Delta\sigma_3$) resulting from the geocell reinforcement, to be calculated using Eq. 2.9. The additional confining pressure was determined by considering factors such as the secant modulus of the geocell material (M) at a specific axial strain (ε) and the initial diameter of the geocell (D).

2.3 SUMMARY

The literature review focuses on the in-depth exploration of two primary categories of stone columns, namely Ordinary Stone Columns and Encased Stone Columns. Through an extensive review of relevant academic studies and research papers, this section presents a comprehensive understanding of the state of knowledge in these areas. It delves into the structural and geotechnical aspects, as well as the performance and behavior of these columns in various applications. This literature review critically summarizes the studies included in each category, highlighting key findings, methodologies, and conclusions.

Chapter 3

NUMERICAL MODELING AND METHODOLOGY

3.1 FINITE ELEMENT ANALYSIS

Finite Element Analysis (FEA) is a widely used computational technique for solving various intricate engineering problems. It involves dividing a structure or system into interconnected elements, which represent the behavior of the actual object. Through the utilization of mathematical models, such as governing physical laws or material properties, FEA solves a system of equations to simulate and predict the system's behavior under different boundary conditions. By discretizing the problem domain, FEA can ascertain stresses, strains, displacements, and other relevant parameters. This method enables engineers and scientists to assess the performance, strength, and durability of structures, components, and materials. FEA finds extensive application in mechanical, civil, aerospace, and automotive engineering, aiding in design optimization, virtual prototyping, and gaining insights into complex phenomena.

3.2 PLAXIS

PLAXIS, an abbreviation for Plane strain and axisymmetric, signifies the geometric types specifically addressed in its original code. It serves as a software application within the field of geotechnical engineering, enabling the performance of finite element analyses (FEA) encompassing deformation, stability, and water flow. Its input procedures facilitate the utilization of advanced output features, allowing for a comprehensive presentation of computational results. The development of the finite element code for PLAXIS 3D took place in 2006 by Brinkgreve and Vermeer, leading to the division of the finite element software into two components: PLAXIS2D and PLAXIS3D. While PLAXIS2D excels in handling plane-strain and axisymmetric problems, PLAXIS3D is better suited for accurately replicating site conditions in FEA.

The primary objective of PLAXIS is to offer a practical analysis tool for geotechnical engineers. Its versatility is evident through the incorporation of various features such as Geogrids, embedded beams, ground anchors, and tunnels, making it a highly flexible and comprehensive geotechnical software package. It includes soil models like Mohr-Coulomb, and Hoek-Brown model. It can also model the behaviour of soft soil, hardening soil, and soft soil creep. Therefore it is capable of capturing the actual behaviour of soil as observed in the field.

3.3 PROBLEM STATEMENT

To study the behaviour of ESC, it becomes imperative to adopt a soil profile and apply a subsequent loading to study the deformation of the improved ground.

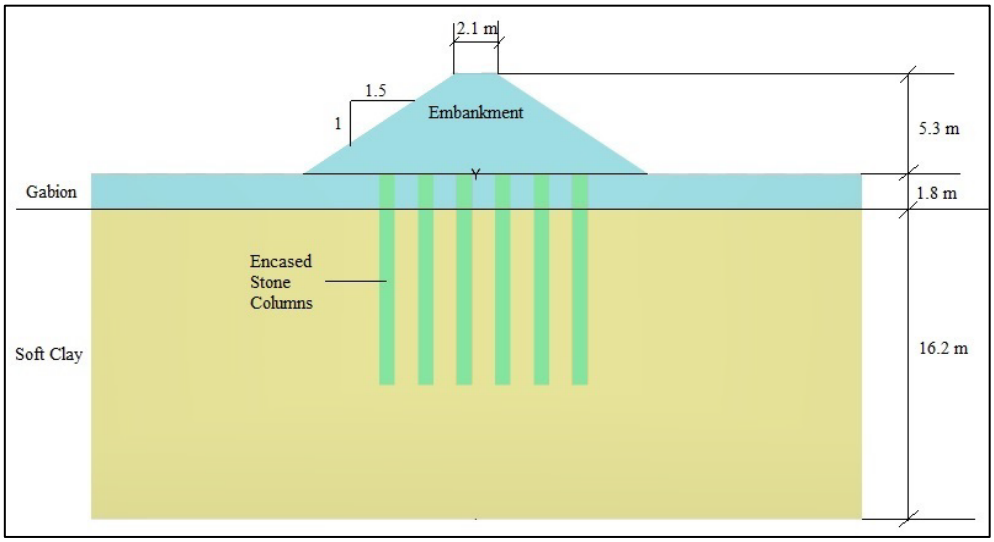

Fig. 3.1 Representative soil profile

Fig. 3.1 illustrates a schematic diagram showcasing the embankment, soil profile, and ground improvement measures. The embankment height is set at 5.3 m, featuring a side slope with a ratio of 1:1.5. To investigate the impact of load increments on the deformation of the improved ground, the density was varied. The ground improvement consists of a 1.8 m thick gabion layer situated above a 16.2 m layer of soft clay. Additionally, Granular Columns with a diameter of 0.8 m and length 11m were implemented as ground improvement measures. All dimensions in this study have been adopted from Hosseinpour (2019). To evaluate the overall performance of the ESC-Gabion system, several of the key parameters have been varied to study their effect on the overall performance. These parameters are, namely, undrained cohesion of the soft-soil, angle of internal friction of the granular column material, spacing of the granular columns, length of encasement, stiffness of the geocell material used in gabion, and stiffness of the encasement geosynthetic.

3.4 USE OF PLAXIS 3D FOR THE PRESENT STUDY.

The numerical simulation of the OSC/ESC involves essential input data, including the properties of the soft clay and granular columns, the length and spacing of the columns, the stiffness of the geosynthetics used, and the properties of the embankment. For the numerical modeling, the finite element analysis software PLAXIS 3D V20 was employed. The process follows a sequential order, beginning with the selection of soil parameters and subsequently creating an appropriate geometry. Once the geometry is established, meshing is performed

based on the desired level of accuracy. Lastly, the type of calculation is determined, and the analysis is executed to generate the desired output.

3.4.1 *Material Model and properties*

The material properties of different materials used for the numerical study have been furnished in Tables 3.1, 3.2, and 3.3.

Table 3.1 Soft soil model properties used for soft clay layers

Soil	**Soil Model**	**γ_{sat} (kN/m^3)**	**ϕ' (°)**	**c' (kPa)**	**C_c**	**C_s**	**k_h (m/d)**	**k_v (m/d)**	**e_0**	**OCR value**
Silty Clay	Soft Clay	14	10	5,10, 15,20	0.98	0.084	1.6×10^{-5}	5.2×10^{-6}	2.81	1.35

Table 3.2 Mohr-Coulomb parameters used for the granular material type

Materials	**Soil Model**	**γ_{sat} (kN/m^3)**	**ϕ' (°)**	**c' (kPa)**	**E' (mPa)**	**k_h (m/d)**	**k_v (m/d)**
Embankment	Mohr Coulomb	28	45	0	53	1	1
Granular Column	Mohr Coulomb	20	30, 35, 40	0	80	10	10
Gabion	Mohr Coulomb	18	30	45	40370, 41770, 42820, 43670	0.2624	0.2624

Table 3.3 Physical Properties of geogrid used

Geogrid	**Stiffness, kN/m**
Encasement Geogrid	1000,1500,2000,2500
Gabion Geogrid	100,150,200,250

The geocell-sand composite has the potential to be considered a comparable soil layer with higher cohesive strength than the surrounded soil. Additionally, the composite retains the same angle of friction as the encased soil. The cohesion induced in the soil (denoted as C_r) is

connected to the rise in confining pressure resulting from geocell reinforcement. This relationship was derived by Madhavi (2007) using the subsequent equation.

$$Cr = \frac{\Delta\sigma_3\sqrt{Kp}}{2} \tag{3.1}$$

where, K_p is the coefficient of passive earth pressure, and $\Delta\sigma_3$ is the additional confinement developed due to the geocell confinement, which can be calculated as

$$\Delta\sigma_3 = \frac{2M[(1-\sqrt{1-\varepsilon})]}{D(1-\varepsilon)} \tag{3.2}$$

Here, ε represents the axial strain upon reaching the failure state, with a designated value of 0.25. The symbol M denotes the secant modulus of the geocell material when subjected to an axial strain of ε. Additionally, D_0 corresponds to the initial diameter of the geocell, with a specific value of 0.2256 meters as adopted in this respective study.

It must also be noted that confining the granular material adds to the Young's modulus of the granular material. Madhavi (2006) proposed the following empirical equation to calculate the Young's Modulus E_g .

$$E_g = 4(\sigma_3)^{0.7}(K_u + 200\bar{M}^{0.16}) \tag{3.3}$$

3.4.2 *Model Configuration*

For numerical simulation, a rectangular slice was chosen beneath the embankment centreline. The zone of interest exhibited two orthogonal planes of symmetry, allowing for modelling only half of the test embankment. Validation studies, included in the later part of the study, showed that the strip model was equally effective in determining the soil behaviour. The utilization of a 3D slice resulted in a significant reduction in calculation time, approximately 46%.

The selected slice was 1 m-wide and included three central encased granular columns, as shown in the plan and 3D strip isometric views depicted in Fig. 3.2 (a) and Fig. 3.2 (b) respectively. To model the soil volume in PLAXIS 3D, 10-node tetrahedral elements were employed to represent the soft clay layers, granular columns, and embankment fill material. These 10-node tetrahedral elements were generated during the 3D mesh generation process. This element type provides a second-order interpretation of displacement while maintaining linearity in pore pressure development, as highlighted in studies by Tandel et al. (2012, 2013) and Brinkgreve and Vermeer (2015).

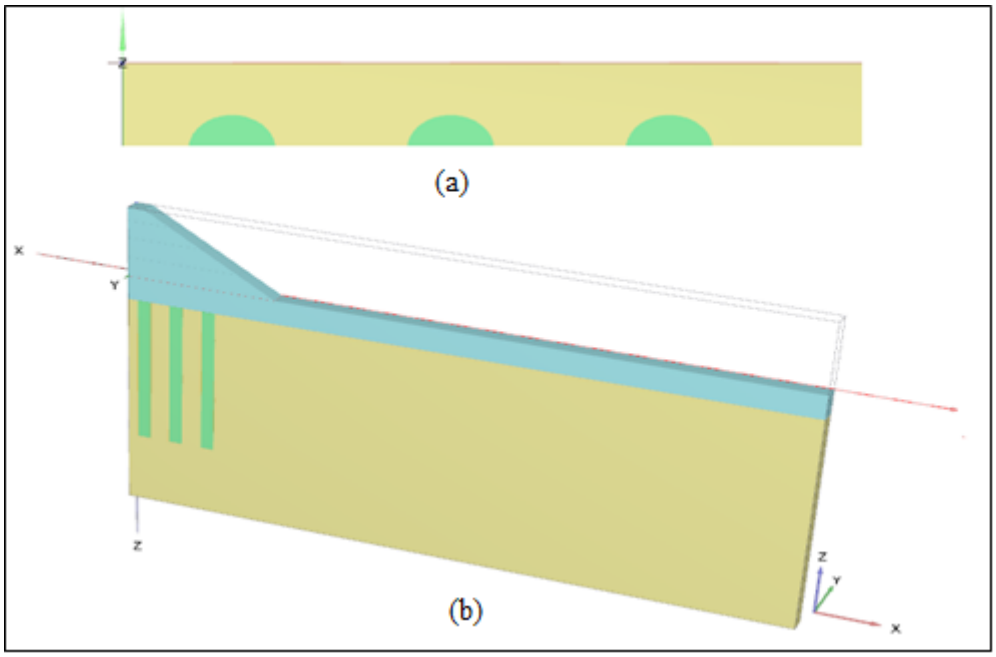

Fig. 3.2 (a)Plan view and (b) Overall Geometrical Model of the ESC-supported Embankment

3.5 METHODOLOGY

The research methodology primarily focuses on the numerical analyses of the gabion-granular column system. The numerical analysis was conducted using advanced geotechnical software, PLAXIS 3D to simulate the behavior of the foundation system in a virtual environment. The Finite Element Method (FEM) was employed to model the complex soil-structure interaction involved. In broader terms, the process of numerical analysis was broken down into five categories:

a) Soil
b) Structures
c) Mesh
d) Flow/Boundary Condition
e) Staged Construction

A flowchart of the numerical modelling sequence have been showcased in Fig. 3.3

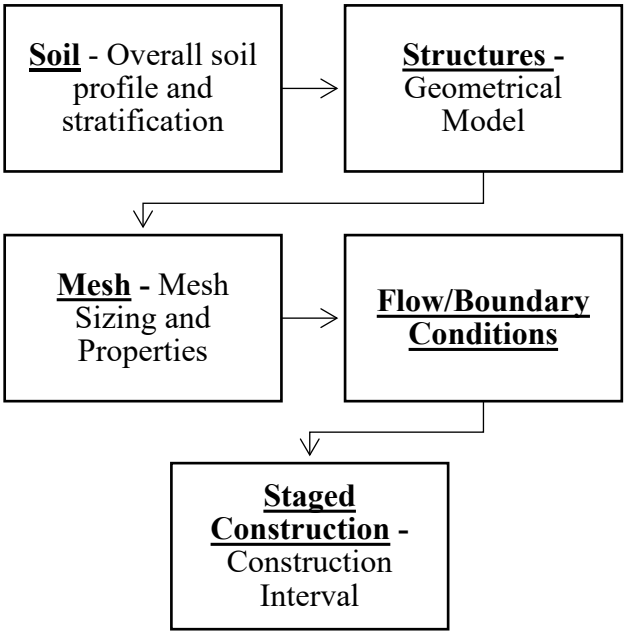

Figure 3.3 Flow chart of the numerical modelling sequence

3.5.1 *Soil*

The numerical modelling begins by defining the soil profile, which includes adding materials and assigning their respective properties. The properties of the soft clay, embankment, and granular column are specified in a Table 3.1, 3.2 and 3.3 respectively. The overall soil stratification, as specified by Hosseinpour (2019), and illustrated in Fig. 3.1 was modelled initially. Also, the soil models to be adopted were finalized at this stage. The water table was specified below the gabion layer, at a depth of 1.8m below the ground surface.

However, an essential consideration in this process is selecting an appropriate soil model. The commonly used primary soil model is the Mohr-Coulomb model. But the limitation of Mohr-Coulomb Model lies in its linear stress-strain relationship. The definite yield point specified in the Mohr-Coulomb model does not match the in-situ behaviour of soft clays. In order to better simulate the compression and consolidation of the soft clay, the soft-soil model was utilized for this specific layer.

Mohr coulomb: Soils exhibit nonlinear behaviour when subjected to changes in stress or strain. The stiffness of soil depends on factors such as stress level, stress path, and strain level. Advanced soil models in PLAXIS incorporate such features to capture complex soil behaviour. However, as a first approximation of soil behaviour, the Mohr-Coulomb model is commonly used due to its simplicity and well-known characteristics.

The Mohr-Coulomb model is a linear elastic perfectly plastic model. The linear elastic part is based on Hooke's law of isotropic elasticity, represented by Young's Modulus (E) and Poisson's ratio (v). The perfectly plastic part is derived from the Mohr-Coulomb failure criterion.

In geotechnical engineering, the Mohr-Coulomb soil model is used to characterize soil behavior. It employs cohesion (c) and the angle of internal friction (φ) to represent shear strength. The model relates shear stress (τ) to normal stress (σ_n) through the equation.

$$\tau = c + \sigma_n \tan \varphi \tag{3.4}$$

When the applied stresses exceed these values, the soil experiences shear failure. Despite its simplicity, the model is widely applied in various engineering analyses.

Soft Soil*:* In geotechnical engineering, the soft soil model is utilized to characterize the behaviour of soft and sensitive soils that demonstrate significant compressibility and deformation under relatively low stress levels. These soils have low shear strength and are susceptible to settlement and consolidation when subjected to external loads. The model takes into account soil compressibility and its response to changes in effective stress.

The Soft Soil Model is defined by the compression index (C_c) and swelling Index (C_s), representing the rates of compression and swelling, respectively. Equations relating the void ratio (e) to effective vertical stress (σ'_v) are used to describe soil behaviour under compression and swelling conditions. While the Soft Soil Model simplifies the understanding of soft soil behaviour, more advanced models might be necessary for detailed analyses in complex situations. The deformation in the soft soil model is governed by the soft soil parameters λ^* and κ^* which are governed by the cam-clay parameters λ and κ, specified by Eqs. 3.4 and 3.5 respectively.

$$\lambda^* = \frac{\lambda}{1+e} \tag{3.5}$$

$$\kappa^* = \frac{\kappa}{1+e} \tag{3.6}$$

However, in PLAXIS, internationally normalized parameters are used to calculate λ^* and κ^* specified by Eqs. 3.6 and Eq. 3.7

$$\lambda^* = \frac{Cc}{2.3(1+e)} \tag{3.7}$$

$$\kappa^* = \frac{2Cs}{2.3(1+e)} \tag{3.8}$$

The coefficients of compression and swelling, C_c and C_s, are obtained from the oedometer test. However, they can also be co-related with the initial void ratio e_0 using various empirical relations. Therefore, in general, when considering the deformation of soft soil, the most crucial parameter involved comes down to be the initial void ratio (e_0).

3.5.2 *Structures*

In the numerical modelling process, after specifying the necessary soil parameters, soil models, and the stratification of the soil layers, the next step involves incorporating the structures into the model. In this study, two structures are considered: the granular column and the embankment.

To model the embankment, a polygon was formulated by defining its coordinates. The polygon essentially represents the footprint or the plan view of the embankment. Once the polygon is defined, it is extruded along a length of 1 meter to create the three-dimensional shape of the embankment. This extrusion process extends the polygon vertically, generating a solid representation of the embankment in the numerical model. Similarly, for the granular column, a semi-circular plate is used as the base representation. The semi-circular shape is extruded vertically to create the three-dimensional representation of the granular column in the model.

For the encasement of the granular column, a semi-circular ring shape is utilized. Like the previous structures, the semi-circular ring is also extruded vertically to generate the three-dimensional encasement shape.

These extrusion processes ensure that the structures have the desired dimensions and are accurately represented in the numerical model. By incorporating the granular column and the embankment as structures, the study can investigate their behaviour and interactions with the surrounding soil under different loading conditions and scenarios.

3.5.3 *Mesh*

As mentioned earlier, the numerical model in this study employs 10-noded tetrahedral elements to discretize the soil volume. To strike a balance between computational efficiency and accuracy, the mesh refinement was set to medium. This decision was made considering the time required for each calculation step.

To control the mesh size and obtain more accurate results in specific areas of interest, a coarseness factor of 1.0 was initially used throughout the model. However, in the vicinity of

the stone columns, where precise vertical deformation values are crucial, the coarseness factor was reduced to 0.5. This local mesh refinement allowed for more detailed analysis and better representation of the behaviour of the soil around the stone columns, as depicted by Fig. 3.4 (a).

Similarly, for the geogrid that encases the granular columns, achieving correct lateral deformation values is essential. Therefore, the coarseness factor was also reduced to 0.5 in the region of the geogrid to ensure accurate modelling of lateral deformations in this specific area, depicted in Fig. 3.4 (b).

By selectively adjusting the coarseness factor, the numerical model strikes a balance between computation time and accuracy. It allows for a more precise analysis in critical regions of interest, such as the stone columns and the geogrid encasement, while still maintaining computational efficiency in other areas. This approach helps to obtain reliable and detailed results for the behaviour of the soil and structures under different loading and boundary conditions, leading to a better understanding of the overall system response and more informed engineering decisions.

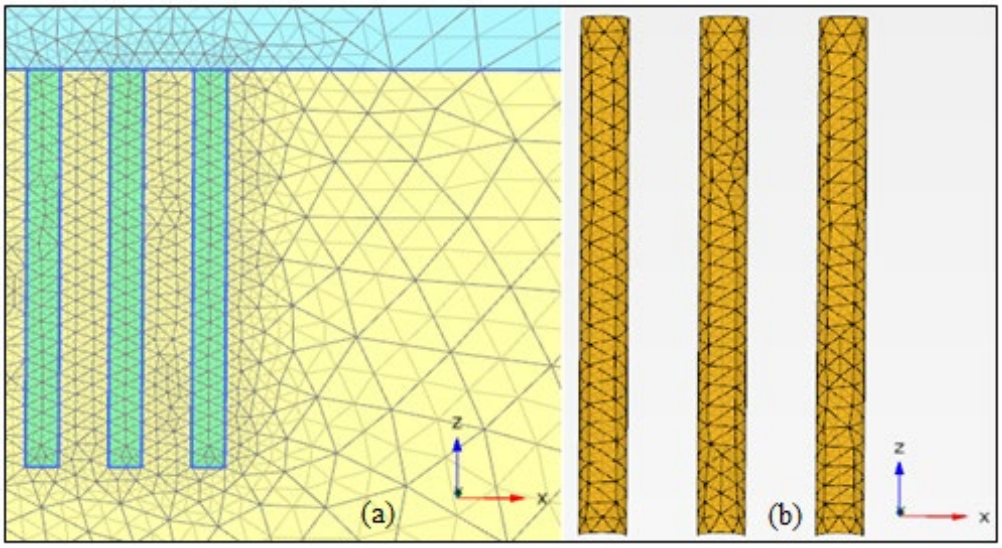

Figure 3.4 (a) Local Mesh Refinement around granular columns and (b) Encasement mesh pattern

3.5.4 *Boundary/Flow Conditions*

In Plaxis 3D, boundary conditions are essential for defining the behaviour of the model at the edges of the analysed domain. They play a crucial role in simulating realistic soil-structure interaction and capturing the response of the geotechnical system accurately. The boundary conditions provided are specified at each boundary (X_{min}, X_{max}, Y_{min}, Y_{max}, Z_{min}, and Z_{max}) and are described as follows:

1. *X_{min} Boundary*:

The "Fixity" at the X_{min} boundary was set to "Roller," which meant that the structure's translation is constrained in the X-direction but allowed deform freely in the vertical direction (along Z axis). This condition simulates a situation where the structure is supported on a roller, permitting horizontal movement but preventing any vertical movement or settlement. The "Flow Allowance" is specified as "Closed," which means that no water flow is allowed through this boundary. This reiterates the fact that the X_{min} represents the axis of symmetry and no flow takes place through it.

2. *X_{max} Boundary*:

At the X_{max} boundary, the "Fixity" is set to "Fixed," indicating that the structure is completely restrained in all directions (translation and rotation) along the X-axis. This condition models a situation where the structure is anchored or connected to an external constraint, preventing any movement or rotation in the X-direction. The "Flow Allowance" is specified as "Open," which means that water flow is allowed through this boundary. It represents a permeable condition, allowing water to enter or exit the analysis domain through this boundary.

3. *Y_{min} Boundary*:

The "Fixity" at the Ymin boundary is set to "Roller," similar to the Xmin boundary, allowing horizontal translation but preventing vertical movement or settlement. The "Flow Allowance" is specified as "Closed," just like the Xmin boundary, indicating an impermeable condition where no water flow is allowed through this boundary.

4. *Y_{max} Boundary*:

At the Y_{max} boundary, the "Fixity" is set to "Roller," providing horizontal translation but restricting vertical movement or settlement. The "Flow Allowance" is specified as "Closed," making it impermeable to water flow.

5. *Z_{min} Boundary*:

The "Fixity" at the Z_{min} boundary is set to "Free," meaning there is no constraint on translation or rotation in any direction. This boundary condition simulates a condition where the model is free to deform without any external restraint. The "Flow Allowance" is specified as "Open," allowing water to flow freely through this boundary, representing a fully permeable condition.

6. *Z_{max} Boundary*:

At the Z_{max} boundary, the "Fixity" is set to "Fixed," meaning the structure is completely constrained in all directions (translation and rotation) along the Z-axis. This condition models a situation where the structure is anchored or connected to an external constraint, preventing any movement or rotation in the Z-direction. The "Flow Allowance" is specified as "Open," allowing water to flow freely through this boundary, representing a fully permeable condition.

The boundary conditions, collectively summarised in Table 3.4 help to define the behaviour of the geotechnical system within the Plaxis 3D analysis, considering different degrees of freedom and permeability at each boundary.

Table 3.4 Boundary conditions for numerical model

Boundary	**Fixity**	**Flow allowance**
X_{min}	Roller	Closed
X_{max}	Fixed	Open
Y_{min}	Roller	Closed
Y_{max}	Roller	Closed
Z_{min}	Free	Open
Z_{max}	Fixed	Open

3.5.5 *Staged Construction*

The initial step of the analysis involved establishing the geostatic stress state and pore water pressures. To define the initial stress state, a lateral earth pressure condition known as "at-rest" was adopted in the model. However, it's important to note that the effects of stone column installation were not considered in this initial state, as in general, the embankment construction takes place only after 3-4 years of stone column construction. To simulate the load application, the analysis proceeded with the current construction stage of the test embankment, followed by a consolidation period of six months. The calculation steps included activating the clusters

corresponding to the different layers of the embankment. This allowed for a detailed examination of how each layer responded to the loading and consolidation process.

During the analysis, specific consolidation intervals were defined between the different construction stages. These intervals were necessary to study the dissipation of excess pore pressures within the saturated soft soil layer over time. The consolidation intervals helped understand how the soil's pore water pressure gradually reduced during the consolidation process. The details of the embankment construction, including the construction stages, consolidation periods, and layer-specific information, are presented in Table 3.5.

In summary, the analysis's initial step involved establishing the geostatic stress state and pore water pressures, using an "at-rest" lateral earth pressure condition. Subsequent stages simulated the embankment construction and consolidation process, considering specific time intervals to study pore pressure dissipation. The provided Table 3.5 contains a comprehensive summary of the embankment construction details and consolidation steps.

Table 3.5 Details of calculation phases

Calculation Phase	**Type of analysis**	**Embankment Height (m)**	**Interval (d)**	**Event**
Initial phase	K_0 Procedure	-	-	Initial Stress State
Phase 1	Consolidation	1.5	3	Construction + Consolidation
Phase 2	Consolidation	1.5	10	Consolidation
Phase 3	Consolidation	3	2	Construction + Consolidation
Phase 4	Consolidation	3	32	Consolidation
Phase 5	Consolidation	4.3	2	Construction + Consolidation
Phase 6	Consolidation	4.3	14	Consolidation
Phase 7	Consolidation	5.3	2	Construction + Consolidation
Phase 8	Consolidation	5.3	180	Consolidation

3.6 NUMERICAL MODELS FOR GENERAL COMPARISION

It is evident from the existing literature that encasing a granular column significantly improves the performance of weak soil. Adding a load distribution platform in the form of gabion further aides in spreading the load and further improves the performance of the system. To quantify the degree improvement imparted by encasing the granular columns and presence of Gabions, three distinct numerical models were formulated as specified in Table 3.6.

Table 3.6 Model properties for general comparision

Sl. No.	Name	Soil Properties	Description
1.	ESC with Gabion	c= 15kN/m^2, ϕ_{clay} = 10°, ϕ_{sc} = 40°, spacing=2m c/c, J_{sc}=1500 kN/m J_{gab}=150 kN/m (E=42000 kN/m^2)	Standard case wherein the granular columns are encased, and gabion is present.
2.	OSC with gabion	c= 15kN/m^2, ϕ_{clay} = 10°, ϕ_{sc} = 40°, spacing=2m c/c, J_{sc}= NA J_{gab}=150 kN/m (E=42000 kN/m^2)	The granular columns are uncased, but gabion is present.
3.	ESC without Gabion	c= 15kN/m^2, ϕ_{clay} = 10°, ϕ_{sc} = 40°, spacing=2m c/c, J_{sc}=1500 kN/m J_{gab}= NA	The granular columns are encased but any form of load bearing platform (gabion) is absent.

In the first model, the granular columns were encased, and a load distribution platform provided in the form of gabion. In order observe the influence of the granular column encasement, uncased granular columns were used in the second model. However, the gabion was kept constant from the first model. In the third model, the gabion was excluded but the granular columns were encased in this case. The relative degree of improvements is presented in the form of vertical and lateral displacement and pore water pressure. Also, the stress distributions are plotted to effectively visualize the zones of higher stresses.

3.7 NUMERICAL MODELS FOR PARAMETRIC VARIATION

The primary aim of this research was to identify and analyse the key factors that exerted the most significant influence on the performance of the Gabion-Granular Column system. To achieve this objective, a comprehensive parametric study was conducted. This study involved systematically varying different parameters to understand their individual and collective impacts on the system's performance.

To carry out this investigation, a series of models were prepared, each representing different combinations of the parameters under consideration.The corresponding outcomes are presented in a tabulated (Table 3.7) format for easy reference and understanding.

Table 3.7 Details of Numerical Models

Expected Outcome	**Constants**	**Variables**	**No. of Models**
Vertical and Lateral Displacement, Pore Water Pressure + Bearing Capacity	Spacing=2m c/c, L_{enc}= 13.75D (full enc.), ϕ_{clay}=10°, J_{sc}= 1500 kN/m, E_{gab}=42000 kN/m²	ϕ_{sc}=30°, 35°, 40° C_{clay} = 5,10,15 and 20 kN/m²	12+12=24
	ϕ_{sc}=40°, L_{enc}= 13.75D (full enc.), ϕ_{clay}=10°, J_{sc} = 1500 kN/m, E_{gab}=42000 kN/m²	spacing=2, 2.4, 2.8 m c/c, C_{clay}= 5,10,15 and 20 kN/m²	12+12=24
	ϕ_{sc}=40° spacing=2m c/c, ϕ_{clay}=10°, J_{sc} = 1500 kN/m, E_{gab}=42000 kN/m²	L_{enc}= 0D, 4D, 8D, 12D, C_{clay} = 5,10,15 and 20 kN/m²	16+16=32
	ϕ_{sc}=40° spacing=2m c/c, J_{sc} = 1500 kN/m, Φ_{clay}=10°, Lenc=Full enc.	J_{gab}= 100, 150, 200, 250 kN/m C_{clay} = 5,10,15 and 20 kN/m²	16+16=32
	ϕ_{sc}=40° spacing=2m c/c, Φ_{clay}=10°, E_{gab}= 42000 kN/m² L_{enc}=Full enc.	J_{sc}= 1000, 1500, 2000, 2500 kN/m C_{clay} = 5,10,15 and 20 kN/m²	16+16=32

Five parameters were selected to observe their influence on the performance of the ESC-gabion foundation performance. These parameters are, namely, undrained cohesion of the soft-soil

$\boldsymbol{C_{clay}}$, angle of internal friction of the granular column material $\boldsymbol{\phi_{sc}}$, spacing of the granular columns, length of encasement $\boldsymbol{L_{enc}}$, stiffness of the geocell material used in gabion $\boldsymbol{J_{gab}}$, and stiffness of the encasement geosynthetic, $\boldsymbol{J_{sc}}$. Total 144 numerical models were formulated in five different series. The soil stratification and the dimension of the granular columns and the embankment were constant throughout all the numerical models.

In the first series, the response of the system on varying the angle of internal friction of the granular column (ϕ_{sc} = 30°, 35°, 40°) was recorded. In the second series, the spacing of the granular columns (spacing = 2, 2.4 and 2.8 m c/c) were varied while keeping the other parameters constant. In third and fourth series, the influence of Length of encasement of the granular columns (L_{enc} =0D, 4D, 8D and 12D) and stiffness of the geocell gabion (J_{gab} = 100, 150, 200 and 250 kN/m) were investigated. Lastly, the influence of adding additional lateral stiffness to the granular column were examined. This was achieved by varying the stiffness of the encasement geogrid (J_{sc}= 1000, 1500, 2000 and 2500 kN/m). Throughout the different numerical models, the shear strength of the soft clay was varied (C_{clay} = 5, 10, 15 and 20 kN/m^2).

The impact of individual parameters on the manifestation of three crucial outcomes; vertical and lateral displacement, pore water pressure, and bearing capacity, was examined. By analyzing the changes in these outputs, whether they showed increase, decrease, or exhibited varying rates of change, the extent of influence each parameter exerted on the ESC-gabion foundation system's overall performance could be gauged.

3.8 SUMMARY

The numerical model adopted for this study has been devised in this chapter. The various components of the numerical model comprise of five different scopes, namely, assigning the soil model, specifying the geometrical model, assigning proper boundary conditions, and finally specifying the construction interval and calculation type. The soft soil model was found to be the best fit for the type of soil used in this study. Also, the meshing was adopted such that finer refinement could be achieved near the granular columns. Finally, the staged construction was specified by assigning the time interval of embankment construction. The results from these numerical tests have been discussed in the following chapter.

RESULTS AND DISCUSSIONS

4.1 INTRODUCTION

The present study focuses on behavior of an ESC-Gabion foundation system under embankment loading. A parametric study is conducted to highlight the influence of each parameter. This chapter presents the results and discussions on obtained data in terms of displacements, pore water pressure and bearing pressures etc.

Numerical investigations were conducted utilizing Mohr-Coulomb's criterion to account for elasto-plastic tendencies in granular materials, embankment, and the gabion structure. However, the soft clay was simulated using the soft-soil (based on Cam-Clay model) model as available in PLAXIS software, as per Hosseinpour (2019). Drained behavior was assumed for all materials in the analyses. It was considered that sufficient time was allowed during the load application, allowing stress concentration and settlement to reach a stabilized state. The initial vertical stress caused by gravity loading was included in the analysis. In PLAXIS, the granular columns are constructed by replacing an equal volume of soft clay with granular materials. Hence, the stress induced by the intrusion of granular columns can be considered as negligible. However, it may vary depending on other methods of Stone Column construction.

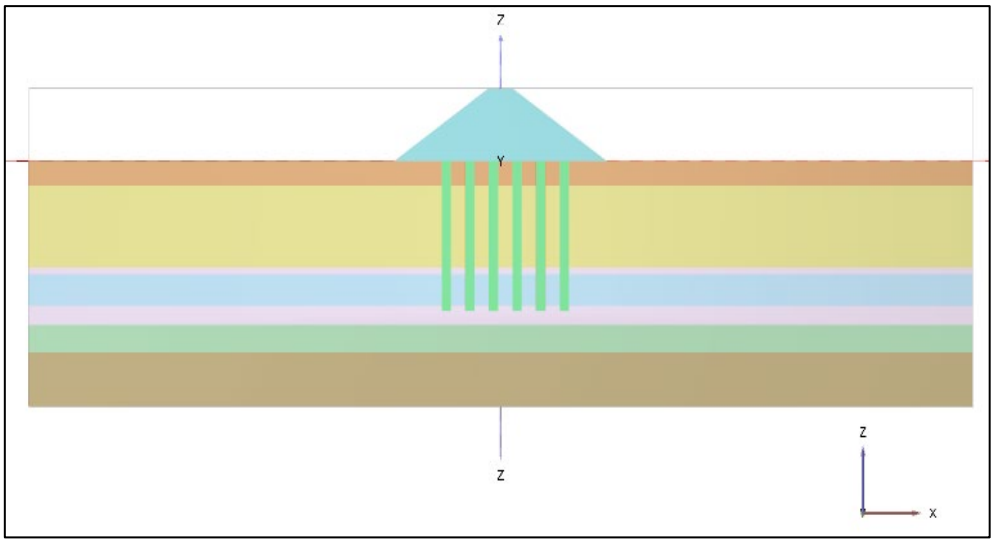

Fig. 4.1 Full embankment model considering Hosseipour's (2019) soil stratification

The adopted model's validation was based on the 3-D strip model created by Hosseinpour et al. (2019) (Fig. 4.2). The comparison of the vertical displacement versus time curve demonstrated strong concurrence. Furthermore, a distinct model was formulated encompassing the entire embankment, as depicted in the Fig. 4.1.

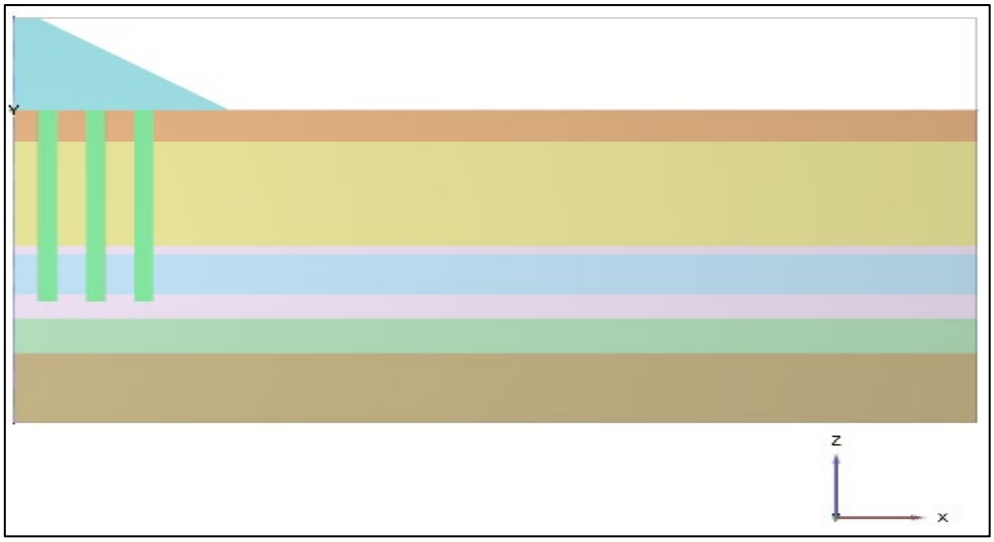

Fig. 4.2 Numerical model of Hosseinpour (2019)

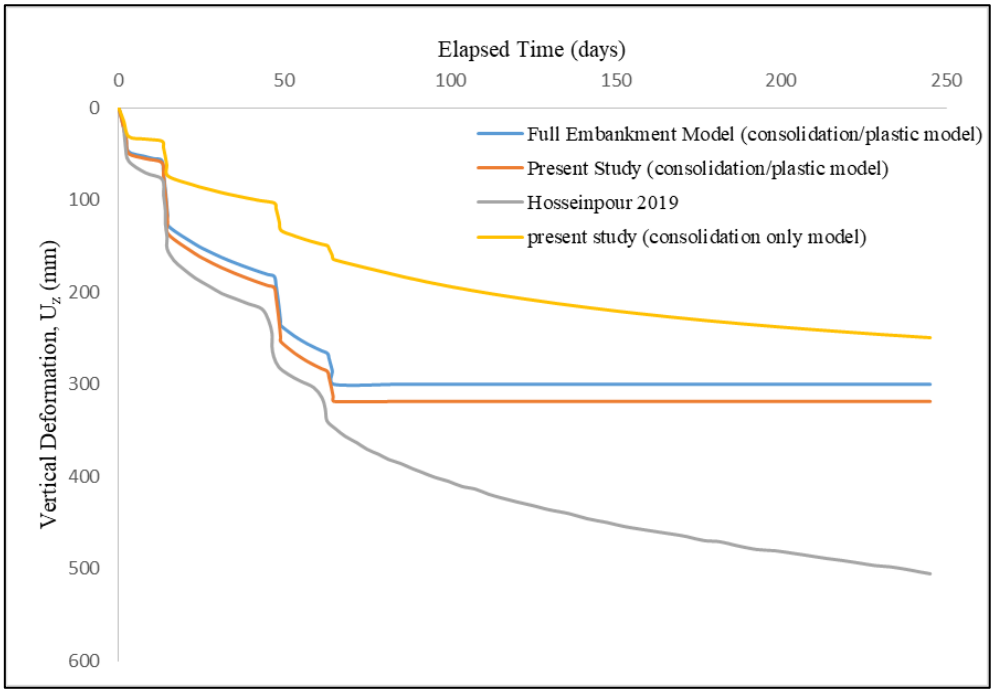

Fig. 4.3 Validation of numerical model with Hosseinpour (2019)

Settlements below the central axis of the embankment, specifically at coordinates (0, 0, -1), were examined and compared to both the full embankment model and the findings presented by Hosseinpour in 2019, as depicted in Fig. 4.3. The analysis revealed that the settlement values deviated no more than 15%, up to the completion of the 65-day construction period. Remarkably, following this construction phase, the settlement exhibited absence of further increase. This phenomenon can be ascribed to the computation methodology employed by Hosseinpour (2019), which primarily focused on consolidation and plasticity as the governing calculation phases. Notably, consolidation is an ongoing process that commences with the

initial application of loading. Consequently, the calculation methodology was consistently changed to "consolidation" for all phases, as specified in the Table 3.5. However, this decision inadvertently led to a reduction of nearly 50% in the final consolidation settlement value.

In summary, the settlements initially displayed an expected increase upon the introduction of load during the embankment construction, followed by a gradual stabilization throughout the successive consolidation phases. It is evident that the numerical simulations accurately projected the observed nature of settlement curve throughout all phases of embankment construction, extending into the post-construction phase.

These observations offer further validation for the chosen model and serve as a solid foundation for the current investigation. Nevertheless, it is important to note that there were modifications made to the soil layering, departing from Hosseinpour's original research. Specifically, the revised model simplified the soil structure, featuring only a single layer of soft clay, with specific details outlined in the Table 3.1. This simplification not only sped up the computational processes but also enhanced the clarity of visualizing the stress distribution within the embankment.

4.2 EFFECT OF ENCASEMENT AND GABION ON OVERALL PERFORMANCE

For the general understanding of the behavior of ESCs and the improvement it offers over OSC, few standard parameters were chosen to represent a numerical model, labelled as “ESC with Gabion” case. The parameters used for this model are exhibited in table 3.6.

A “OSC with Gabion” model and an “ESC without gabion” model were also fabricated with the parameters kept same as the “ESC with Gabion” case. Detailed description of these models have been furnished in section 3.6.

4.2.1 *Excess Pore Water pressure*

One of the prime challenges involved in the improvement of weak clays is to aide in the dissipation of excess pore water pressure, p_{excess} which in turn facilitates consolidation. Stone columns are seen as an effective solution for the above-mentioned problem.

Upon examining the stress contours of all the three cases, as presented in Figs. 4.4, 4.5 and 4.6 respectively, it was seen that the most of the pore pressure built up occurred under the unsupported part of the embankment and the granular columns. The granular columns, both uncased and encased showcased effective dissipation of excess pore water pressure. The dissipation of pore water pressure, as depicted by the blue zone in the stress plot, around the

granular column portrayed that effective consolidation around the zone of influence of the granular columns. Malarvizhi and Illamparuthi (2007) specified that the effective depth of maximum bulging was about 1D (i.e., 0.8m in this case). The intermediate soil between the two bulged columns will undergo extra squeezing and thus pore water pressure developed should also be of higher order. This is clearly evident from the stress profile. The point between the two columns at a depth of 1D below the gabion/embankment was chosen to plot the pore water dissipation curve for clearer understanding (Fig. 4.7).

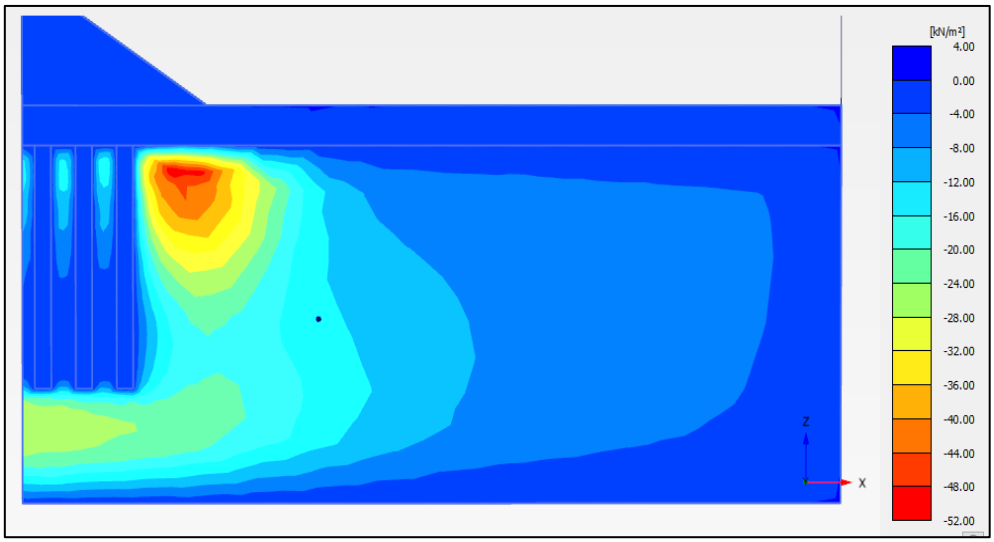

Fig. 4.4 Pore pressure distribution for “OSC with gabion”

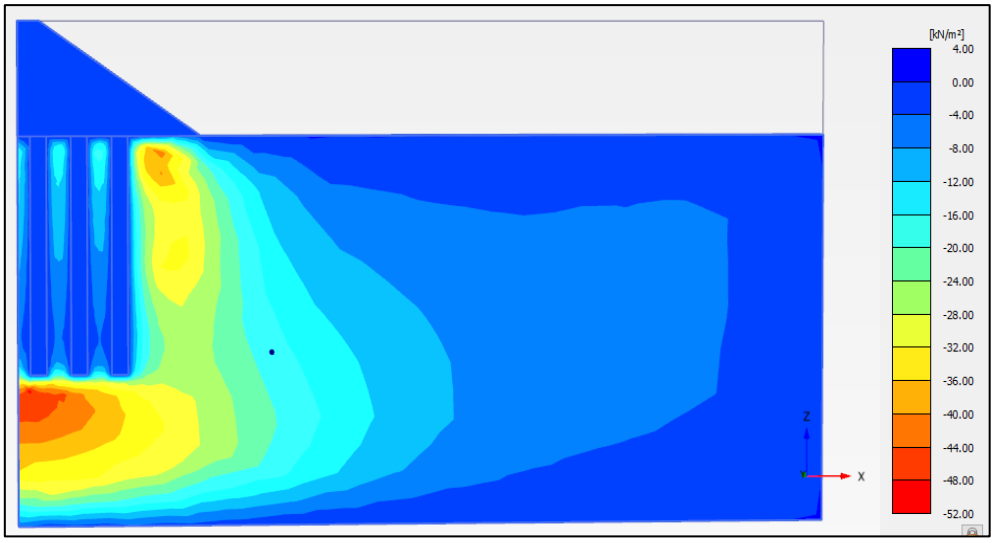

Fig. 4.5 Pore pressure distribution for “ESC without gabion”

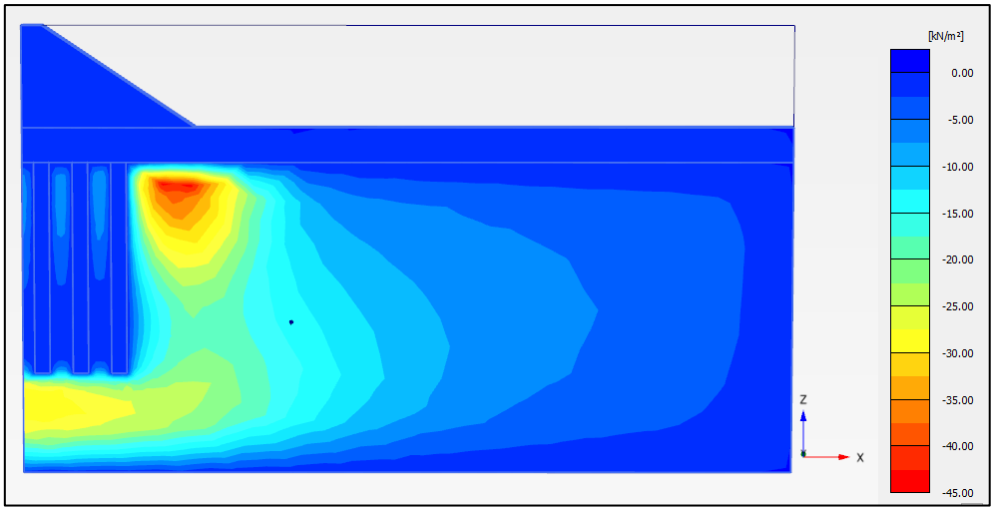

Fig. 4.6 Pore Pressure distribution for "ESC with Gabion"

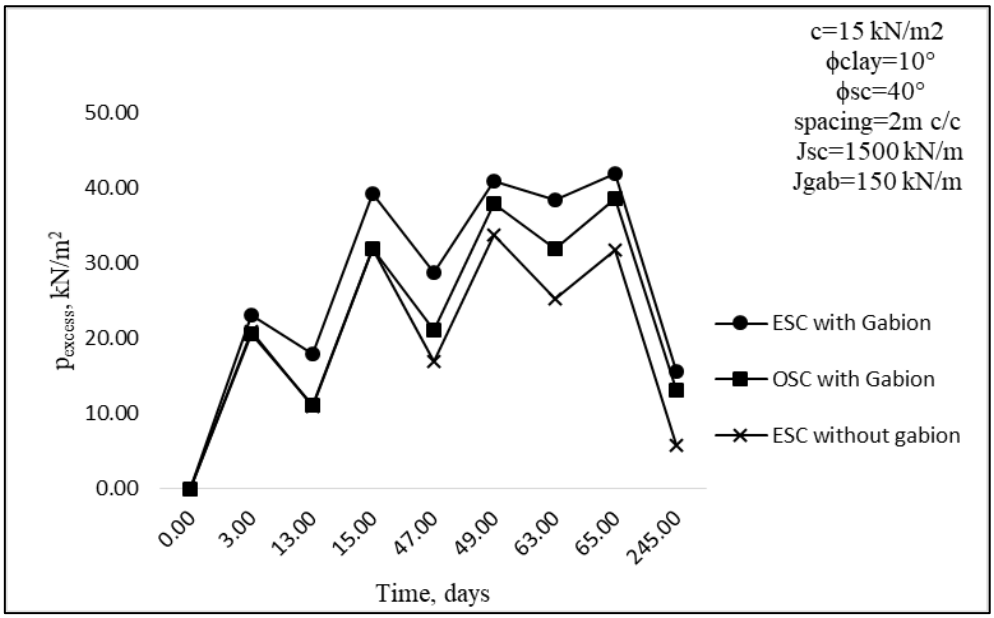

Fig. 4.7 Excess pore water pressure pressure dissipation for different cases

As observed in Fig. 4.7, it was seen that the excess pore pressure experienced a rapid surge when the load was applied, and then it gradually reduced to some extent before the subsequent load application. This surge was observed whenever a layer of embankment was added at day 0, 13, 47 and 63 respectively. In comparison to the "OSC with Gabion" case, the "ESC with Gabion" exhibited a significantly better pore water pressure dissipation performance, registering a 56% improvement and 63% improvement when compared to the "ESC without gabion" case.

Encased Stone Columns exhibit enhanced pore pressure dissipation, showcasing superior effectiveness. The encasement geogrid preserves the structural integrity of the granular column,

allowing the voids to maintain their shape even in weak clay. This retention of void shape ensures that flow paths are maintained, facilitating the ongoing and effective dissipation process.

4.2.2 *Total Vertical Stress*

In order to provide some additional clarity on the degree of improvement imparted by encasement and gabion, an analysis was conducted to examine the distribution of total vertical stress beneath the embankment at the conclusion of the consolidation period. The stress contours, as depicted in Figs. 4.8, 4.9 and 4.10, revealed that, in all three studies, the granular columns experienced the highest levels of stress (indicated by yellow-red range in the stress plot). This observation signifies the accurate definition of the embankment/gabion-column interface and confirms the effective transfer of load from the embankment to the underlying soil via the stone columns.

While comparing the stress plot for all the three cases, it is seen that when gabion is present (“ ESC with Gabion” and “OSC With Gabion”), the vertical stress at the bottom portion of the granular columns are significantly higher (indicated by the red zone). Thus it can be inferred that the gabion helps in distributing the load to deeper strata. In the absence of a gabion, the stress distribution in the granular columns are non-uniform and the inner-most granular column is more critically stress than the outer ones. This again highlights the role of gabion in efficient distribution of load.

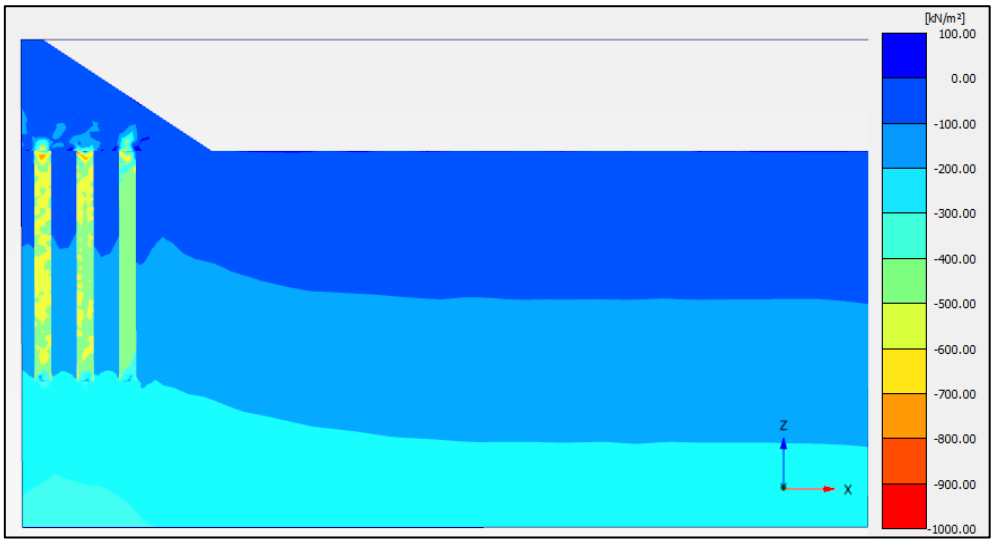

Fig. 4.8: Vertical stress distribution for “ESC without gabion”

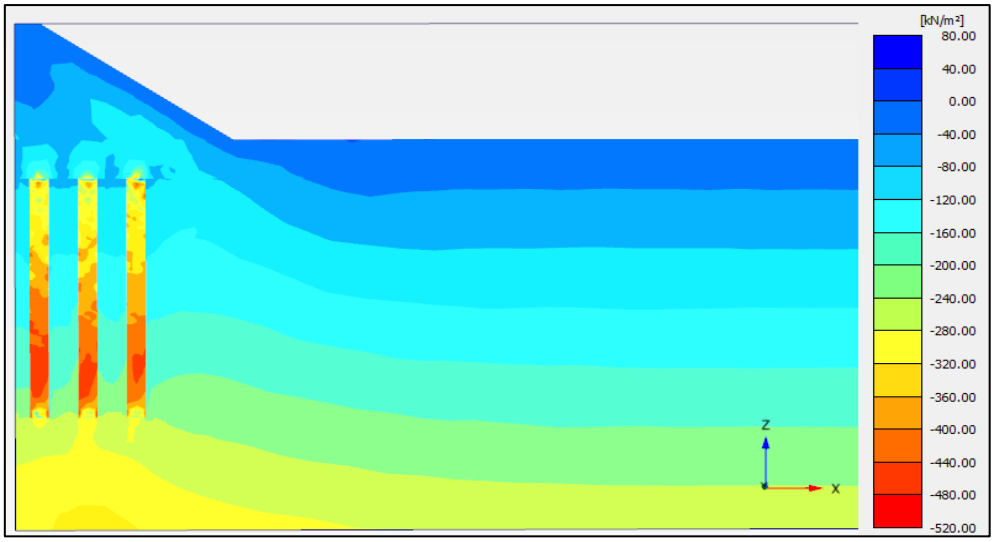

Fig. 4.9: Vertical distribution for "OSC with Gabion"

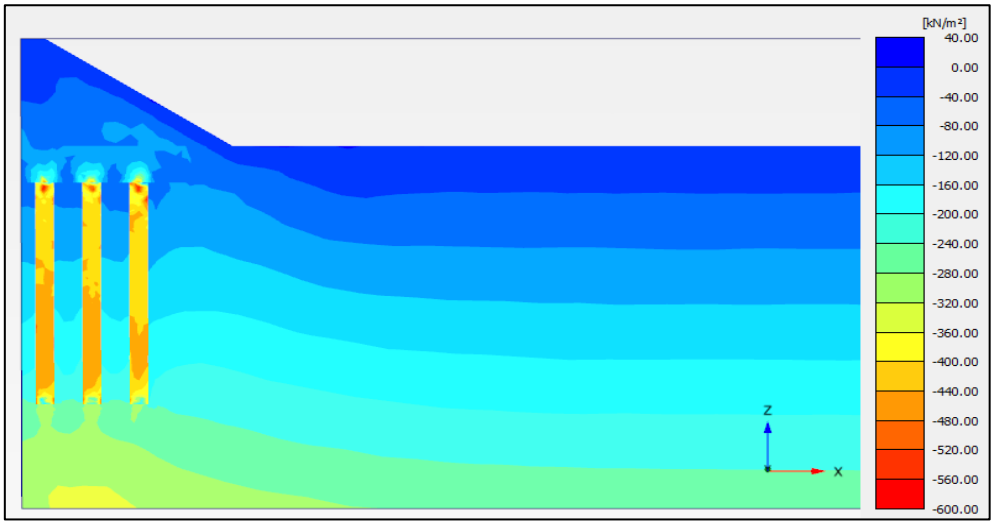

Fig. 4.10 : Vertical Stress distribution for "ESC with Gabion" case.

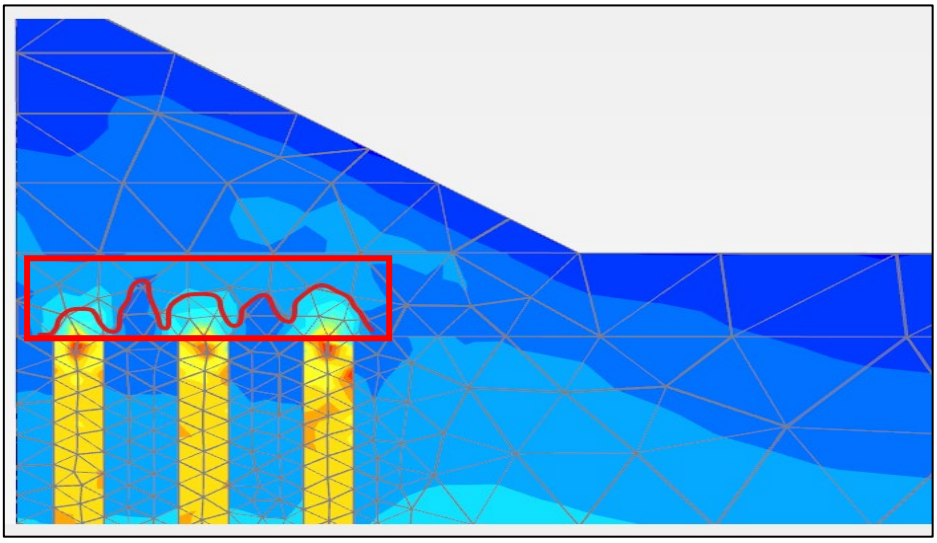

Fig. 4.11 Soil arching action within the gabion

The stress distribution immediately above the granular columns within the gabion structure exhibited an increase in stress levels, as depicted by red lines in Fig. 4.11. This phenomenon, as identified by Hosseinpour (2017), was attributed to the formation of a soil arching zone within the gabion. The soil movement just above the granular column is resisted by shearing stresses developed in the gabion which reduce the pressure on the columns. Thus, the arching effect played a substantial role in sharing a considerable portion of the load emanating from the embankment. Consequently, this led to a reduction in the vertical stresses experienced within the columns themselves.

While studying the influence of gabion in distribution of vertical stress, it was observed that the stress value in the granular column remained relatively lower for "ESC without Gabion" case when compared to other cases wherein gabion was present. This is evident from the yellow-green color in the stress plot (Fig. 4.8).

4.2.3 *Vertical Deformation along Base of Embankment.*

Deformation values were noted along the top most surface of the gabion and a vertical deformation profile was drawn for all of the three concerned cases; namely "ESC with Gabion", "OSC With Gabion" and "ESC Without Gabion". When the stone columns were encased, it resulted in a reduction of 18% in the maximum vertical displacement compared to the scenario without encasement.

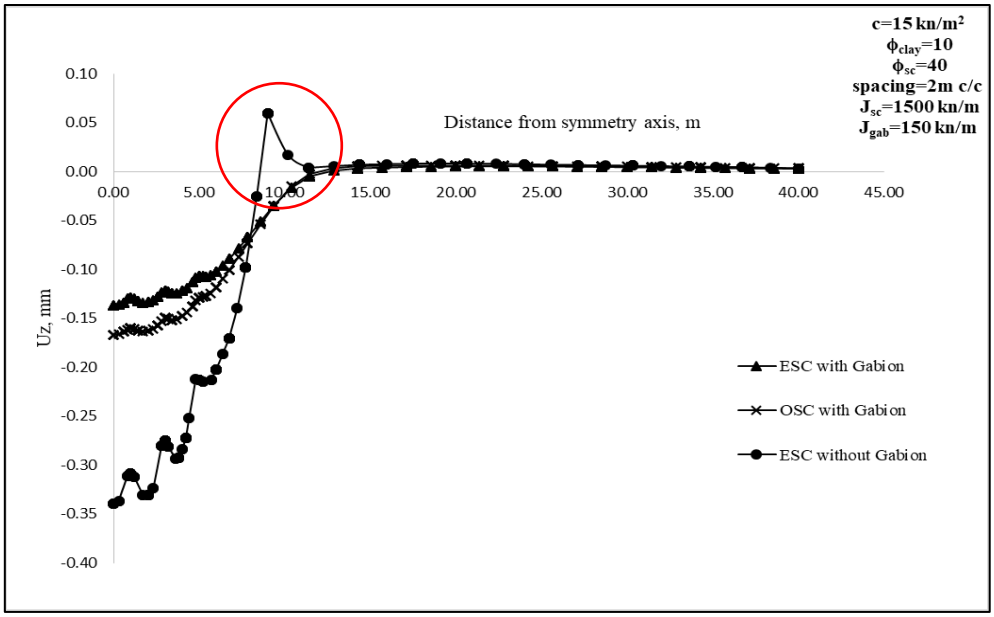

Fig. 4.12 Vertical deformation profile along the base of embankment

Nevertheless, a crucial observation from the deflection profile is that the presence of some form of load distribution platform is absolutely essential when utilizing any type of granular

columns. It is evident from the red circle in Fig. 4.12 that there is significant upheaval where the gabion was not provided, along the embankment's toe end. This abrupt difference in deformation, about 140%, seen for "OSC without gabion" case can be attributed to absence of a proper load distribution platform.

4.2.4 *Lateral Deformation in the Column*

A comparison of the bulging behavior of columns is presented in Fig. 4.13. It was observed that "OSC with Gabion" underwent 45% more bulging compared to the "ESC with Gabion" case. In absence of gabion, the lateral displacement increased by 135% when compared to the "ESC with Gabion". To investigate further on lateral deformation of "ESC without Gabion" case, the horizontal deformation vectors were plotted (Fig 4.14). It was observed that the self-weight of the embankment pushed the soil body further towards right.

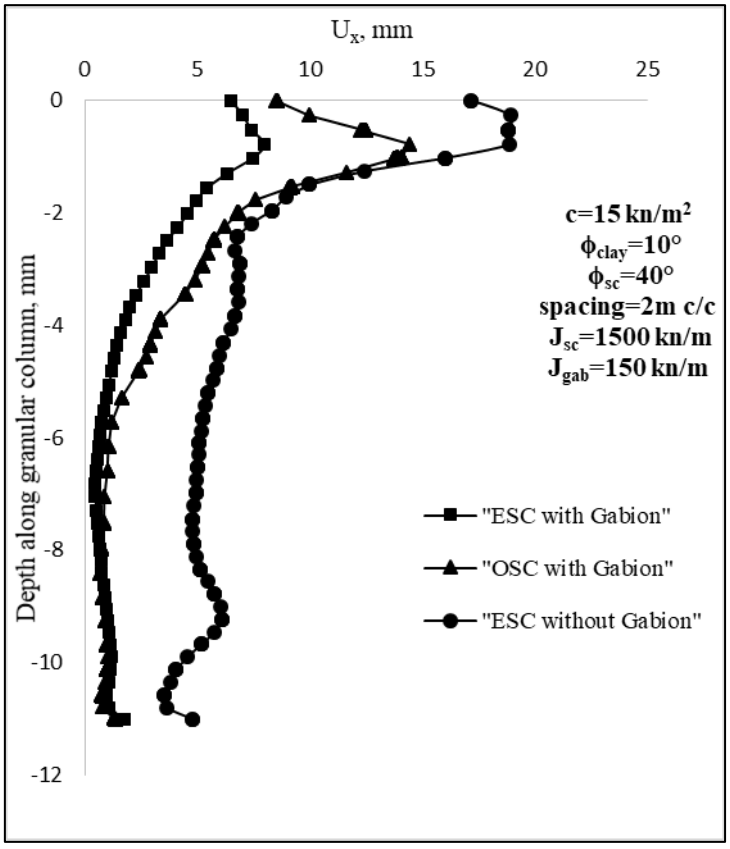

Fig. 4.13 Lateral Deformation profile for various cases

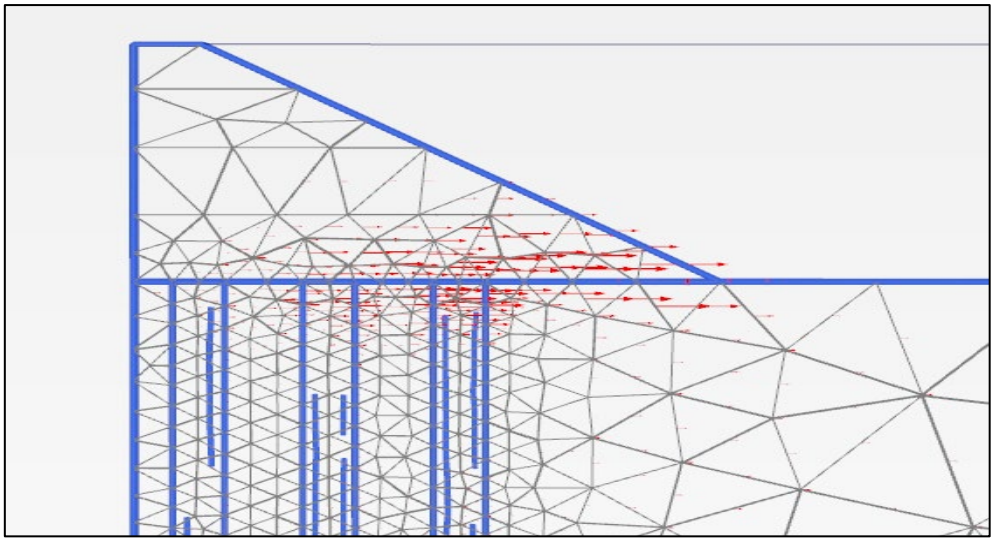

Fig. 4.14 Horizontal deformation vectors in the absence of gabion

4.3 PARAMETRIC STUDY AND ITS EFFECT ON BEARING CAPACITY

The design criteria for Encased Stone Columns (ESCs) are grounded in two fundamental design methodologies. Firstly, the Serviceability Limit State (SLS) approach requires careful consideration of the ESC layout and characteristics to ensure compliance with predefined settlement criteria. Secondly, the Ultimate Limit State (ULS) design, often referred to as the "global" stability design, involves a comprehensive assessment of the potential of failure across the entire embankment-GECs-soft soil system.

In the context of geotechnical analysis, it is essential to select an appropriate model to represent the soil. Within the PLAXIS software, the soft-soil model is specifically custom-made for highly compressible clays. Opting for the Ultimate Limit State design approach may lead to significant deformations, which might not be practical in certain applications. Consequently, it became more suitable to employ the serviceability limit state approach to establish the bearing capacity of the ground reinforced by ESCs. To achieve this, it was necessary to define a permissible settlement value. The permissible settlement value can vary depending on the type of structure under consideration. In the context of this study, a settlement value of 500 mm was adopted This choice aligns with the typical settlement tolerance for liquid storage tanks, which happen to be the most prevalent structures constructed on ground improved by ESCs.

The bearing capacity (q_u) was calculated, as specified in Table 3.7. The models encompassed all the parameters, and the results were plotted to visualize the variation of bearing capacity with the undrained cohesion. The effect of the various parameters are listed below.

4.3.1 *Effect of friction angle, ϕ_{sc}*

The increase in the internal angle of granules, denoted as ϕ_{sc}, should lead to an enhancement in performance. A higher ϕ_{sc} value indicates improved compaction of the granules, thereby reducing lateral strain and consequently yields a greater bearing capacity.

Table 4.1 Bearing capacity comparision for different angle of internal friction, ϕ_{sc}

ϕ_{clay}=10° spacing=2mc/c E_{gab}=42000kN/m² J_{sc}=1500 kN/m full enc.					
ϕ_{sc} = 30°		ϕ_{sc} = 35°		ϕ_{sc} = 40°	
c (kN/m²)	q_u (kN/m²)	c (kN/m²)	q_u (kN/m²)	c (kN/m²)	q_u (kN/m²)
5	177.55	5	190.8	5	201.4
10	196.1	10	209.35	10	222.6
15	212	15	224.72	15	239.56
20	225.25	20	237.705	20	254.4

Table 4.1 lists the data obtained from the numerical models. The obtained plot shows similar results as expected with the bearing capacity, q_u increasing with the friction angle. As evident, the rise in q_u is almost uniform across the values of ϕ_{sc}.

4.3.2 *Effect of spacing*

The bearing capacity expected to rise as the spacing between the stone columns decreases. A close arrangement of granular columns provides improved structural support. Nevertheless, it's essential to acknowledge that there is a threshold spacing. The limitation is due to the insufficient soil-volume for the required development of the soil-column interaction as described by Bachus and Barsdale (1983).

Table 4.2 lists the data obtained from the numerical models. As predicted earlier, q_u increases with the reducing spacing.

Table 4.2: Bearing capacity comparision for different spacing

ϕ_{clay} =10° ϕ_{sc}=40° E_{gab}=42000 kN/m² J_{sc}=1500 kN/m full enc.							
spacing= 1.6 m c/c (2D)		spacing= 2 m c/c (2.5D)		spacing= 2.4 m c/c (3D)		spacing= 2.8 m c/c (3.5D)	
c (kN/m²)	q_u (kN/m²)	c (kN/m²)	q_u (kN/m²)	c (kN/m²)	q_u (kN/m²)	c (kN/m²)	q_u (kN/m²)
5	209.1	5	201.4	5	199.81	5	194.245
10	228.26	10	222.6	10	219.42	10	212.53
15	245.1	15	239.56	15	234.79	15	227.9
20	257.5	20	254.4	20	247.51	20	240.62

4.3.3 *Effect of Length of Encasement, L_{enc}*

In the study, the bearing capacity of stone-columns are noted to be increaseing as the length of encasement, L_{enc} increases. The encasement provides confinement to the column by mobilizing the tensile force in the geosynthetics, which reduces the lateral stress and strain developed inside the granular column. Uncased granular columns mostly fail by bulging. Providing a confinement in the form of encasement helps reduce this bulging. Increasing the length of this encasement increases the overall confinement of the granular material. However, since the bulging mostly occurs at the top half of the granular column, the length of encasement can be curtailed by some extent at the end.

Data was obtained from Table 4.3. The data justify the common perception of the effect of encasement length . However, the decrease in the rate of change in performance from Lenc=8D to L_{enc}=12D suggests that the effect of encasement length is not as prominent above 8D as below it. This is due to the fact that the maximum hoop stress in the ESC develops only within the length of 1D (Malavizhi and Ilamparuthi 2007) and thus encasement below it doesn't play much role in increasing q_u .

Table 4.3 Bearing capacity comparision for different length of encasement, L_{enc}

ϕ_{clay} =10° ϕ_{clay}=40° Egab=42000 kN/m^2 Jsc=1500 kN/m spacing=2mc/c							
L_{enc}=0D		L_{enc}=4D		L_{enc}=8D		L_{enc}=12D	
c (kN/m²)	q_u (kN/m²)	c (kN/m²)	q_u (kN/m²)	c (kN/m²)	q_u (kN/m²)	c (kN/m²)	q_u (kN/m²)
5	176.49	5	190.27	5	198.22	5	204.58
10	194.51	10	210.41	10	219.95	10	226.84
15	211.47	15	226.31	15	236.38	15	243.8
20	225.25	20	240.62	20	250.69	20	258.64

4.3.4 *Effect of the Gabion Geocell stiffness, J_{gabion}*

Increased stiffness in the gabion implies greater flexural rigidity of the gabion, resulting in a larger portion of the applied load being supported by the gabion by the virtue of arching action. Consequently, this augmentation should lead to an increase in the overall bearing capacity of the system. Thus it can be postulated that increasing the stiffness would increase the load bearing capacity of the ESC-Gabion system.

Table 4.4 Bearing capacity comparision for geocell stiffness of gabion, J_{gabion}

ϕ_{clay}=10° $\phi_{sc=}$ 40° spacing=2mc/c J_{sc}=1500 kN/m full enc.							
Geocell stiffness= 100 kN/m		Geocell stiffness= 150 kN/m		Geocell stiffness= 200 kN/m		Geocell stiffness= 250 kN/m	
c (kN/m²)	q_u (kN/m²)	c (kN/m²)	q_u (kN/m²)	c (kN/m²)	q_u (kN/m²)	c (kN/m²)	q_u (kN/m²)
5	200.87	5	201.4	5	201.93	5	202.195
10	222.6	10	223.13	10	223.395	10	223.925
15	240.09	15	240.09	15	240.62	15	240.726
20	253.605	20	253.87	20	254.4	20	254.93

Table 4.4 lists the data obtained from the numerical models. From the data listed, it was observed that the stiffness of gabion, J_{gabion} didn't play much role in increasing the bearing capacity of the system. The bearing capacity, q_u remained almost unchanged with increasing gabion stiffness, J_{gabion} .

In the study, it is found that though alterations in the stiffness of the gabion encasement (J_{gabion}) can exert an influence on factors such as lateral deformation and settlement of the stone column, their impact on the ultimate bearing capacity is typically limited. The ultimate bearing capacity is primarily determined by the interaction between the soil and the structure, along with the load transfer mechanisms related to the confinement of intermediate spaces. Influence of the stiffness-modification of the gabion encasement is not significant in altering the confinement. Thus, it is likely that this leads to the notable deviations from the expected outcome.

4.3.5 *Effect of geosynthetic stiffness, J_{sc}*

The bearing capacity of a ESC foundation system increases in correspondence with the stiffness of the encasement geosynthetic, denoted as J_{sc}. The reason being, elevating the stiffness of the encasement enhances the confinement of the granular materials. It's important to note that bearing strength is derived from both the resistance to vertical and lateral deformation.

Table 4.5 Bearing capacity comparision for different stiffness of encasement geogrid, J_{sc}

ϕ_{clay}=10° ϕ_{sc} =40° spacing=2mc/c E_{gab}=42000 kN/m² full enc.							
J_{sc} = 1000 kN/m		J_{sc} = 1500 kN/m		J_{sc} = 2000 kN/m		J_{sc} = 2500 kN/m	
c (kN/m²)	q_u (kN/m²)	c (kN/m²)	q_u (kN/m²)	c (kN/m²)	q_u (kN/m²)	c (kN/m²)	q_u (kN/m²)
5	194.51	5	201.665	5	206.7	5	212
10	215.71	10	223.13	10	229.596	10	235.85
15	232.405	15	240.355	15	247.086	15	253.764
20	245.92	20	254.4	20	261.82	20	268.445

Table 4.5 furnishes the data to understand the variation of J_{sc} with c. It was observed that the bearing capacity increases steadily with the increase in geosynthetic stiffness J_{sc} as anticipated.

4.4 PARAMETRIC STUDY AND ITS EFFECT ON MAXIMUM VERTICAL DEFORMATION

Plots of vertical deflections were generated to gain a more detailed understanding of how the ESCs were performing. To achieve this, a specific point located along the line of symmetry directly beneath the gabion at coordinates (0, 0, 1.8) was selected and a parametric analysis carried out. The deflection at the point is inversely proportional to the bearing capacity.

4.4.1 *Effect of friction angle, ϕ_{sc}*

Table 4.6 lists the data obtained from the numerical analysis. It was observed that the clear gap between the plots signified the influence ϕ_{sc} exerts over the performance of ESCs. However, this influence reduces as the *c* increases.

Table 4.6: Bearing capacity comparision for different angles of internal friction, ϕ_{sc}

ϕ_{clay}=10° spacing=2mc/c E_{gab}=42000 kN/m² J_{sc}=1500 kN/m full enc.					
ϕ_{sc} =30°		ϕ_{sc} =35°		ϕ_{sc} =40°	
c (kN/m²)	U_z (mm)	c (kN/m²)	U_z (mm)	c (kN/m²)	U_z (mm)
5	254.5	5	211.7	5	179
10	212.6	10	185	10	156.7
15	190.7	15	165.7	15	141.5
20	173.5	20	151.8	20	130.2

4.4.2 *Effect of spacing*

Table 4.7 Vertical deformation comparision for different spacing

ϕ_{clay} =10° ϕ_{sc}=40° E_{gab}=42000 kN/m² J_{sc}=1500 kN/m full enc.							
spacing=1.6mc/c (2D)		spacing= 2mc/c (2.5D)		spacing= 2.4mc/c (3D)		spacing= 2.8mc/c (3.5D)	
c (kN/m²)	U_z (mm)	c (kN/m²)	U_z (mm)	c (kN/m²)	U_z (mm)	c (kN/m²)	U_z (mm)
5	160.5	5	179	5	195.3	5	209.1
10	139.5	10	156.7	10	171.9	10	184.3
15	125.2	15	141.5	15	154.7	15	165.6
20	115.1	20	130.2	20	141.8	20	151.8

From the data obtained from Table 4.7, it can be inferred that Vertical deformation diminishes as the spacing reduces. As the spacing between granular columns reduces, the effective confinement of soil in between the granular columns increases. This increase in state of confinement further increases the bearing capacity of the entire system. Nonetheless, it

becomes apparent that this impact diminishes in significance as the spacing reduces from 2.4m c/c to 2mc/c and subsequently to 1.6m c/c.

4.4.3 *Effect of Length of Encasement, L_{enc}*

In previously covered aspects, it was seen that the bearing capacity of ESC improved with increasing the length of encasement, L_{enc}.. Keeping in accordance with the previously recorded data, increasing L_{enc} results in a decrease of the vertical deformation underneath the embankment. Vertical Deformation values for different L_{enc} were tabulated in Table 4.8.

Table 4.8 Vertical deformation comparision for encasement length, L_{enc}

ϕ_{clay} =10° ϕ_{sc}=40° Egab=42000 kN/m^2 Jsc=1500 kN/m spacing=2mc/c							
Lenc=0D		Lenc=4D		Lenc=8D		Lenc=12D	
c (kN/m²)	U_z (mm)	c (kN/m²)	U_z (mm)	c (kN/m²)	U_z (mm)	c (kN/m²)	U_z (mm)
5	222.8	5	189.1	5	177.7	5	173.5
10	191.9	10	163.9	10	154.2	10	149.8
15	171.5	15	146.8	15	136.3	15	131.8
20	156.8	20	134.1	20	124.1	20	119.6

As anticipated, a substantial enhancement is observed when transitioning from OSC (i.e., Lenc = 0D) to ESC (i.e., Lenc = 4D). Nevertheless, it was observed that there is minimal alteration when extending the encasement length from 8D to 12D. This phenomenon is likely attributed to the fact that the maximum bulging of the column occurs at approximately 1D (equivalent to 0.8 meters), and thus encasing top most portion only exerts maximum influence.

4.4.4 *Effect of the Gabion Geocell stiffness, J_{gabion}*

As evident from the existing literature, the vertical deformation is rises with an increase in the stiffness of the gabion geocell, represented as J_{gabion}. A higher stiffness in the gabion signifies enhanced flexural rigidity, which translates to a greater portion of the applied load being borne by the gabion. The Deformational values for values were tabulated in Table 4.9

Table 4.9 Vertical deformation comparision for different stiffness of gabion geocell, J_{gabion}

ϕ_{clay} =10° ϕ_{sc}=40° Jsc=1500 kN/m spacing=2mc/*c* full enc.							
J_{gabion} =100 kN/m		J_{gabion} =150 kN/m		J_{gabion} =200 kN/m		J_{gabion} =250 kN/m	
c (kN/m²)	U_z (mm)	c (kN/m²)	U_z (mm)	c (kN/m²)	U_z (mm)	c (kN/m²)	U_z (mm)
5	179.8	5	179	5	178.4	5	178
10	157.3	10	156.7	10	156.4	10	155.9
15	142.1	15	141.5	15	141.4	15	140.9
20	130.6	20	130.2	20	129.9	20	129.7

As evident from the furnished data,, the stiffness of the gabion has a negligible impact on the stone column's performance. This trend is similarly mirrored in the context of vertical deformation.

4.4.5 *Effect of geosynthetic stiffness, J_{sc}*

The geosynthetic stiffness affects the hoop stress on the encasement. This develops a passive resistance to the granular column, which is otherwise asserted by the surrounding soil. This lateral pressure results in an upward thrust. The values for Vertical deformation for different values of J_{sc} were tabulated in Table 4.10

Table 4.10 Vertical deformation comparision for different stiffness of encasement geogrid, J_{sc}

ϕ_{clay} =10° ϕ_{sc} =40° E_{gab}=42000 kN/m² spacing=2mc/c full enc.							
J_{sc} = 1000 kN/m		J_{sc} = 1500 kN/m		J_{sc} = 2000 kN/m		J_{sc} = 2500 kN/m	
c (kN/m²)	U_z (mm)	c(kN/m²)	U_z (mm)	c(kN/m²)	U_z (mm)	c(kN/m²)	U_z (mm)
5	189.5	5	179	5	170.7	5	164.1
10	165.4	10	156.7	10	149.8	10	144.1
15	149.1	15	141.5	15	135.5	15	130.5
20	136.9	20	130.2	20	124.6	20	120

4.5 PARAMETRIC STUDY AND ITS EFFECT ON MAXIMUM LATERAL DEFORMATION IN ENCASEMENT (COLUMN BULGING)

The lateral deformation in the encasement occurs due to the bulging of column. It is a crucial phenomenon as far as granular columns are concerned. Bulging of columns compacts the soil in between and helps it attain a certain degree of bearing capacity. A parametric study was conducted to determine the parameters which mostly affected the bulging of columns.

4.5.1 *Effect of friction angle, ϕ_{sc}*

Numerical analysis was performed and Lateral Displacement, U_x were calculated for different values of $\phi_{sc.}$. The values were tabulated in Table 4.11.

Table 4.11 Lateral deformation comparision for different angles of internal friction, ϕ_{sc}

ϕ_{clay}=10° spacing=2mc/c E_{gab}=42000 J_{sc}=1500 kN/m full enc.					
ϕ_{sc}=30°		ϕ_{sc} =35°		ϕ_{sc} =40°	
c (kN/m²)	U_x (mm)	c (kN/m²)	U_x(mm)	c (kN/m²)	U_x(mm)
5	14.99	5	12.49	5	10.17
10	12.18	10	10.51	10	8.84
15	10.68	15	9.377	15	7.97
20	9.67	20	8.52	20	7.322

Raising the angle of friction enhances the interlocking of particles, leading to a reduction in lateral deformation with an increase in ϕsc. This dilation of the granular material consequently diminishes the lateral spread of the granular materials. The obtained data depicted a sharp rise for ϕsc for c = 5 kN/m^2. This is due to the lack of passive resistance from the clay of weak shear strength (c = 5 kN/m^2).

4.5.2 *Effect of spacing*

The Table 4.12 showcases the values of Lateral Displacement for different values of spacing. The data was in agreement to the findings from previous sections. Widening the spacing between ESCs results in reduced confinement of the soil between the columns. This leads to a decrease in passive resistance to the granular materials, subsequently causing an increase in dilation.

Table 4.12 Lateral deformation comparision for different spacing

ϕ_{clay} =10° ϕ_{sc}=40° E_{gab}=42000 kN/m^2 J_{sc}=1500 kN/m full enc.							
spacing=1.6mc/c		spacing=2mc/c		spacing=2.4mc/c		spacing=2.8mc/c	
c (kN/m^2)	U_x (mm)	c (kN/m^2)	U_x (mm)	c (kN/m^2)	U_x (mm)	c (kN/m^2)	U_x (mm)
5	6.47	5	10.17	5	14.84	5	19.03
10	5.99	10	8.84	10	12.31	10	15.41
15	5.6	15	7.97	15	10.71	15	13.09
20	5.23	20	7.322	20	9.58	20	11.91

4.5.3 *Effect of the Gabion Geocell stiffness, J_{gabion}*

From previous sections, it was observed that the stiffness of gabion did not impart much on bearing capacity or vertical displacement. The values of Lateral deformations against different values of J_{gabion} in Table 4.13.

Table 4.13 Lateral deformation comparision for different stiffness of gabion geocell, J_{gabion}

ϕ_{clay} =10° ϕ_{sc}=40° Jsc=1500 kN/m spacing=2mc/*c* full enc.							
J_{gabion}=100 kN/m		J_{gabion}=150 kN/m		J_{gabion}=200 kN/m		J_{gabion}=250 kN/m	
c (kN/m^2)	U_x (mm)	c (kN/m^2)	U_x (mm)	c (kN/m^2)	U_x (mm)	c (kN/m^2)	U_x (mm)
5	10.22	5	10.17	5	10.11	5	10.1
10	8.88	10	8.84	10	8.83	10	8.8
15	8.01	15	7.97	15	7.91	15	7.94
20	7.38	20	7.322	20	7.312	20	7.29

Similar to its impact on bearing capacity and vertical deformation, the stiffness of the gabion has a minimal influence on the lateral displacement of the encasement. This behavior is

primarily because the primary role of the gabion is to assist in load distribution and does not significantly affect the individual performance of an ESC.

4.5.4 *Effect of geosynthetic stiffness, J_{sc}*

Increasing the stiffness of the encasement, J_{sc} increases the resultant hoop tension which should be result in reduced Lateral Deformation, U_x . The values of lateral deformation against different values of J_{sc} were tabulated in Table 4.14.

Table 4.14 Lateral deformation comparision for different stiffness of encasement geogrid, J_{sc}

ϕ_{clay} =10° ϕ_{sc} =40° E_{gab}=42000 kN/m^2 spacing=2mc/c full enc.							
Jsc=1000 kN/m		Jsc=1500 kN/m		Jsc=2000 kN/m		Jsc=2500 kN/m	
c (kN/m^2)	U_x (mm)	c (kN/m^2)	U_x (mm)	c (kN/m^2)	U_x (mm)	c (kN/m^2)	U_x (mm)
5	11.78	5	10.17	5	8.98	5	8.1
10	10.2	10	8.84	10	7.84	10	7.06
15	9.2	15	7.97	15	7.05	15	6.33
20	8.437	20	7.322	20	6.45	20	5.78

The data obtained were in agreement to the findings of existing literature. Stone material dilates and lateral strain in the stone column induces hoop tension in the encasement, which results in radial compression in stone column. The hoop tension developed depends on the stiffness of geogrid and it offers a passive resistance to the stone column, which is otherwise offered by the surrounding soil. The lateral pressure thus developed results in an upward thrust. The hoop tension developed in the encasement increases with the stiffness of the geogrid. Hence, the lateral deformation reduces.

4.6 SUMMARY

The results from the numerical models have been extensively analyzed and presented in this chapter. Three distinct models, namely “ESC with Gabion”, “OSC with Gabion” and “ESC without Gabion” were formulated. The results were presented in the form of deformation; horizontal and vertical, pore water pressure and total vertical stress. It became evident that the encasement and gabion both played crucial role in efficient load distribution and pore pressure dissipation. Furthermore, the data from the parametric study were presented in the form of bearing capacity and deformation; lateral and vertical. This helped is gauging the influence of each parameter over the performance of the ESC-Gabion foundation system.

CONCLUSIONS, LIMITATIONS AND FUTURE SCOPES OF STUDY

This study aims to provide a comprehensive analysis using FE analysis with PLAXIS3D. The problem geometry was modeled as a 3D strip in PLAXIS. Axis-symmetric model could have been considered in place of 3D Strip model. However, axis-symmetric models are more suitable when modelling a singular granular column. A parametric study was performed to analyze the impact of various factors such as the properties of the soft soil (c and ϕ), angle of friction of the stone column material (ϕ_{sc}), length of encasement, column spacing, geogrid and gabion stiffness, and embankment material density.

5.1 CONCLUSION

The following conclusion can be drawn from the present study:

1) From the extensive literature review done as a part of this study, it was found out that a range of factors impacted the effectiveness of this granular columns. These factors include column dimensions, length, spacing, native soil strength, column material strength, and geosynthetic stiffness in case of ESCs. The dimensions are kept under check by adapting suitable spacing/dia and length/dia ratios which fall around 2-3D and 10-15D respectively. The friction angle of the granular is adapted within an effective range of 30-45°, with occasional occurrences of higher friction angle. The geosynthetic encasement shall be such designed that the size of the aperture doesn't exceed the maximum nominal effective size of the granular materials.
2) The presence of a gabion has a limited impact on the performance of an individual ESC. However, when considering the entire ESC-soft clay system, the gabion's presence becomes crucial. Without the gabion, there was improper load distribution, resulting in ground upheaval along the embankment's side. Additionally, the dissipation of pore water pressure was less effective, leading to higher pore water pressure observed at the end of the consolidation period.
3) Encasing the granular column with the geogrid increases the overall performance of the ESC. The parametric study shows that the increase in stiffness of encasement reduces the settlement and increases the bearing capacity of the entire system
4) As L_{enc} increases, the performance in terms of vertical deformation and bearing capacity improves. However, it is to be noted that upon increasing the length of encasement above 8D, the effect was much less prominent.

5) The angle of shearing resistance of column material affects the performance of ESC. Higher efficiency of ESC can be achieved if the column material is compacted well to achieve high angle of shearing resistance.
6) Numerical studies confirmed the bulging mechanism of stone column. The bulging of stone column is effective up to the depth of 4 times the diameter of the column, with maximum bulging taking place at around 1D which is in conformity with classical theories of Hughes and Withers (1974) and Greenwood (1970) and the present experimental study. Furthermore, it can also be concluded that maximum hoop tension force in the encasement is developed at a depth of 1D.
7) Encasing the stone column increases the stress concentration on the column, thereby reducing the load on clay, consequently reducing the settlement. The parametric study shows that the settlement reduction in the ESC is about 18% of OSC bed for identical conditions.
8) The staged construction methodology provides an effective way to ensure consolidation in saturated weak clay. The pore pressure increases during load application and reduces steadily when left for consolidation. ESC provide better pore water pressure dissipation when compared to OSC.
9) Reducing the gap between the ESC improve the performance of the treated ground. However, this effect is much less prominent when the spacing reduced below 2.5D (2 m c/c).

5.2 LIMITATIONS

The scope of this study is limited, and the following are some the shortcomings of this study:

1) This a numerical study only. Physical data is absent.
2) This study is limited to ϕ_{clay} = 10°.
3) Only 4 values length of encasement, L_{enc} = 0D, 4D, 8D, 12D
4) The length of the ESC has been kept constant in this study.
5) The soil profile adopted in this study is uniform and homogenous. Soil stratification has been ignored in this study.

5.3 FUTURE SCOPE OF THE STUDY

The limitations of this study can be overcome with further research. The potential areas of consideration can be:

1) Developing a physical model to validate the numerical data.
2) Spanning this study for different values of ϕ_{clay} and L_{enc}
3) Adopting stratified soil conditions for the study.
4) Incorporating L/D ratio among one of the parameters of study.

REFERENCES

1. Aboshi, H. "The compozer-a method to improve characteristics of soft clay by inclusion of large diameter sand columns." *Proceedings, International Conference on Soil Reinforcements: Reinforced Earth and Other Techniques*. Vol. 1. 1979.
2. Alamgir, Miura, et al. "Deformation analysis of soft ground reinforced by columnar inclusions." *Computers and Geotechnics* 18.4 (1996): 267-290.
3. Ambily, A. P., and Gandhi,S.R. "Behavior of stone columns based on experimental and FEM analysis." *Journal of geotechnical and geoenvironmental engineering* 133.4 (2007): 405-415.
4. Barksdale, R D., and Bachus, R.C. *Design and construction of stone columns, vol. I*. No. FHWA/RD-83/026; SCEGIT-83-104. Turner-Fairbank Highway Research Center, 1983.
5. Baumann, V., and Bauer, G. E. A.. "The performance of foundations on various soils stabilized by the vibro-compaction method." *Canadian Geotechnical Journal* 11.4 (1974): 509-530.
6. Brinkgreve, R. B. J., Broere, W and Waterman,D "Plaxis, Finite element code for soil and rock analyses, users manual." *The Netherlands* 2006.
7. Chummar, Verghese, A. "Ground improvement using stone columns: problems encountered." *ISRM International Symposium*. OnePetro, 2000.
8. Datye, K. R., and Nagaraju, S.S "Installation and testing of rammed stone columns." *Proceedings of IGS specialty session, 5th Asian Regional Conference on Soil Mechanic and Foundation Engineering, Bangalore, India*. 1975.
9. Fattah, M. Y., Majeed. Q "A study on the behaviour of geogrid encased capped stone columns by the finite element method." *GEOMATE Journal* 3.5 (2012): 343-350.
10. Gao, J.J, et al. "Settlement behavior of soft subgrade reinforced by geogrid-encased stone column and geocell-embedded sand cushion: A numerical analysis." *Advances in Civil Engineering* 2020 (2020): 1-11.
11. Ghionna, V., and Jamiolkowski, M "Colonne di ghiaia." *X Ciclo di conferenze dedicate ai problemi di meccanica dei terreni e ingegneria delle fondazioni metodi di miglioramento dei terreni. Politecnico di Torino Ingegneria, atti dell'istituto di scienza delle costruzioni* 507 . 1981.
12. Goughnour, R. R., and BAYUK, A.A. "A field study of long term settlements of loads supported by stone columns in soft ground." 1979.
13. Greenwood, D. A., and Kirsch, K. "Specialist ground treatment by vibratory and dynamic methods." *Piling and ground treatment*. Thomas Telford Publishing, 1984. 17-45.
14. Hosseinpour, I, Soriano, C, and Almeida, M.S.S "A comparative study for the performance of encased granular columns." *Journal of Rock Mechanics and Geotechnical Engineering* 11.2 (2019): 379-388.
15. Hosseinpour, I, Riccio M., and Almeida, M.S.S. "VERIFICATION OF A PLANE STRAIN MODEL FOR THE ANALYSIS OF ENCASED GRANULAR COLUMNS." *Journal of GeoEngineering* 12.4. 2017.
16. Hughes, J. M. O., and Withers, N.J. "Reinforcing of soft cohesive soils with stone columns: 18F, 9R. GROUND ENGNG. V7, N3, MAY, 1974, P42–49." *International Journal of Rock Mechanics and Mining Sciences & Geomechanics Abstracts*. Vol. 11. No. 11. Pergamon, 1974.
17. Hughes, J. M. O., Withers, N. J. and D. A. Greenwood. "A field trial of the reinforcing effect of a stone column in soil." *Geotechnique* 25.1 (1975): 31-44.
18. Latha, G.M, and Rajagopal, K "Parametric finite element analyses of geocell-supported embankments." *Canadian Geotechnical Journal* 44.8 (2007): 917-927.

19. Malarvizhi, S. N. "Comparative study on the behavior of encased stone column and conventional stone column." *Soils and foundations* 47.5 (2007): 873-885.
20. McKenna, J. M., Eyre, W. A. and Wolstenholme, D. R. "Performance of an embankment supported by stone columns in soft ground." *Geotechnique* 25.1 (1975): 51-59.
21. Mitchell, J.K., and Huber, T.R "Performance of a stone column foundation." *Journal of Geotechnical Engineering* 111.2 (1985): 205-223.
22. Kenneth, M.J "Soil improvement-state of the art report." *Proc., 11th Int. Conf. on SMFE*. Vol. 4. 1981.
23. Wood, M, D., Hu, W, and Nash, D.F.T. "Group effects in stone column foundations: model tests." *Geotechnique* 50.6 (2000): 689-698.
24. Murugesan, S., and Rajagopal, K "Studies on the behavior of single and group of geosynthetic encased stone columns." *Journal of Geotechnical and Geoenvironmental Engineering* 136.1 (2010): 129-139.
25. Nayak NV, Foundation design manual, Dhanapathi Rai publications (P) Ltd, Fourth ed, 1991
26. Ng and Tan , "Simplified and homogenization method in stone column". Soils and Foundations The Japanese Geotechnical Society ,2014.
27. Priebe, Heinz J. "The design of vibro replacement." *Ground engineering* 28.10 (1995), 31–37
28. Pulko, Boštjan, Bojan Majes, and Janko Logar. "Geosynthetic-encased stone columns: analytical calculation model." *Geotextiles and geomembranes* 29.1 (2011): 29-39.
29. Raithel, M. "To the bearing and deformation behaviour of geosynthetic-encased sand-columns" (in German). Series „Geotechnics", University of Kassel, No. 6., 1999
30. Raithel, M, and Kempfert, H.G. "Calculation models for dam foundations with geotextile coated sand columns." *ISRM International Symposium*. ISRM, 2000..
31. Rajagopal and Jayapal, "Encased Columnar Inclusions in Soft Grounds - A Review", Geotechnical Engineering Journal of the SEAGS & AGSSEA Vol. 49 No.1 March 2018 ISSN 0046-5828, 2018
32. Rajagopal and Mohapatra, "Analysis of Failure Mechanism of Geosynthetic-Encased Stone Column Supported Embankments", GeoAmericas 2016 –The 3rd Pan-American Conference on Geosynthetics, 2016
33. Shahu, J. T., Madhav, M. R., and Hayashi, S. "Analysis of soft ground-granular pile-granular mat system." *Computers and Geotechnics* 27.1 (2000): 45-62.
34. Tandel, Y.K., Solanki, C.H and Desai, A.K. "3D FE Analysis of an Embankment Construction on GRSC and Proposal of a Design Method." *International Scholarly Research Notices,* 2013.
35. Thorburn, S. "Building structures supported by stabilized ground." *Geotechnique* 25.1 (1975): 83-94.
36. Van Impe, W., and Silence, P. "Improving of the bearing capacity of weak hydraulic fills by means of geotextiles." *International conference on geotextiles*, 1986.
37. Vinoth, M., Prasad, P.S and Guru Vittal, U.K. "Performance analysis of PLAXIS models of stone columns in soft marine clay." *Geotechnics for Transportation Infrastructure: Recent Developments, Upcoming Technologies and New Concepts, Volume 2*. Springer Singapore, 2019.